DEPARTMENT OF
ECOLOGY
State of Washington

# Sources of Fine Particles in the Wapato Hills-Puyallup River Valley $PM_{2.5}$ Nonattainment Area

April 2010
Publication No. 10-02-009

## Publication and Contact Information

This report is available on the Department of Ecology's website at www.ecy.wa.gov/biblio/1002009.html .

For more information contact:

Air Quality Program
P.O. Box 47600
Olympia, WA 98504-7600

Phone: 360-407-6821

Washington State Department of Ecology - www.ecy.wa.gov

| | |
|---|---|
| o Headquarters, Olympia | 360-407-6000 |
| o Northwest Regional Office, Bellevue | 425-649-7000 |
| o Southwest Regional Office, Olympia | 360-407-6300 |
| o Central Regional Office, Yakima | 509-575-2490 |
| o Eastern Regional Office, Spokane | 509-329-3400 |

*If you need this publication in another format, please contact the Air Quality Program at (360) 407-6800. If you have a hearing loss, call 711 for Washington Relay Service. If you have a speech disability, call 877-833-6341.*

# Sources of Fine Particles in the Wapato Hills-Puyallup River Valley $PM_{2.5}$ Nonattainment Area

*by*

*David Ogulei, PhD, PE*

Air Quality Program
Washington State Department of Ecology
Olympia, Washington

*This page is purposely left blank*

# Table of Contents

# List of Figures and Tables

Page

## Figures

# Tables

# Acknowledgements

This report represents a collection of significant contributions from a number of individuals within the Department of Ecology and Puget Sound Clean Air Agency. The author of the report would like to especially thank the following people for their contribution to this study:

- Ranil Dhammapala, Department of Ecology Air Quality Program
- Katherine Himes, Puget Sound Clean Air Agency
- Doug Schneider, Department of Ecology Air Quality Program
- Sarah Rees, Department of Ecology Air Quality Program
- Jeff Johnston, Department of Ecology Air Quality Program

# Executive Summary

## Purpose

This report provides information to policy makers about the sources of fine particle air pollution in Washington's Wapato Hills-Puyallup River Valley nonattainment area.

## Background information

States monitor air quality in different areas to find out how much pollution is in the air. When an area violates a federal health-based air quality standard, the federal Clean Air Act requires the Environmental Protection Agency (EPA) to classify the area's air quality. EPA can make one of three designations for an area based on a state's recommendation:

- Attainment (meeting a standard)
- Nonattainment (failing to meet a standard)
- Unclassifiable (not enough information to designate)

## Fine particle pollution in the Wapato Hills-Puyallup River Valley area

On November 13, 2009, EPA formally designated part of Pierce County in Washington (the Wapato Hills-Puyallup River Valley area) as nonattainment. The designation took effect December 14, 2009. This area is nonattainment for the 2006 National Ambient Air Quality Standard (NAAQS) for 24-hour $PM_{2.5}$. $PM_{2.5}$ is fine particles that are less than 2.5 micrometers in size. This pollutant can have many serious health effects.

## Effects of a nonattainment designation

In addition to the health effects of air pollution, nonattainment designations can have both environmental and economic consequences for communities in and around the nonattainment area.

When an area is designated nonattainment, the state must develop a State Implementation Plan (SIP) and submit it to EPA within three years. The SIP is a plan for bringing the area back into attainment as quickly as possible. The SIP must include an attainment demonstration showing what actions the state will take to control air pollution, and how these actions will lead to attainment.

## Analysis of $PM_{2.5}$ sources

To determine how to control a pollutant, the Washington Department of Ecology (Ecology) needs to understand the pollutant's sources. Ecology identified the main sources of $PM_{2.5}$ in the Wapato Hills-Puyallup River Valley area by using receptor modeling techniques to analyze

existing $PM_{2.5}$ speciation data. The data were collected from January 2006 to May 2009 using the Speciation Trends Network (STN) sampling protocols in South Tacoma, Washington.

The results of this analysis indicate that the most significant sources of $PM_{2.5}$ in the nonattainment area, in order of their overall average contributions, are:

- wood smoke (45%)
- secondary particles (25%)
- motor vehicles (13%)
- industrial emissions (6%)
- fugitive dust (4%)
- fireworks (2%)
- oil combustion and ships (1%)
- fresh and processed sea salt (4%)

## Conclusions

Wood smoke is the single most important source of $PM_{2.5}$ in the Wapato Hills-Puyallup River Valley nonattainment area. Wood smoke contributed more than half of the $PM_{2.5}$ on most days in the winter, as well as on days when $PM_{2.5}$ levels were the highest. The total amount of wood smoke probably comes from a combination of wood stoves and other wood-fired home heating devices. Outdoor burning is not likely to contribute significantly to $PM_{2.5}$ in this area, because the area surrounding the sampling site is classified as an Urban Growth Area (UGA), where outdoor burning is prohibited.

Although wood smoke emissions were responsible for the majority of the $PM_{2.5}$ pollution on most days, average contributions from wood smoke and local industry appear to have declined each year since 2006. A similar decline was not observed with other sources or with the $98^{th}$ percentile values of the 24-hour wood smoke concentrations.

# 1.0 INTRODUCTION

Numerous health effect studies have shown that exposure to elevated concentrations of fine particles that are less than 2.5 micrometers in aerodynamic diameter ($PM_{2.5}$) causes adverse health effects, including cardiovascular and respiratory effects in sensitive populations (e.g., Pope, 1996; Lewtas, 2007; Huang and Ghio, 2009). Most $PM_{2.5}$ found in the ambient air results from direct emissions from stationary and mobile emission sources, and secondary particles formed through atmospheric reactions.

On October 17, 2006, the United States Environmental Protection Agency (EPA) strengthened the 24-hour $PM_{2.5}$ national ambient air quality standards (NAAQS) from 65 micrograms per cubic meter ($\mu g/m^3$) to 35 $\mu g/m^3$, but retained the annual $PM_{2.5}$ NAAQS at 15 $\mu g/m^3$ (71 FR 61144). The revised 24-hour $PM_{2.5}$ standard became effective on December 18, 2006. To attain this 24-hour standard, the 3-year average of the $98^{th}$ percentile of 24-hour $PM_{2.5}$ concentrations at each population-oriented monitor within an area must not exceed 35 $\mu g/m^3$.

On November 13, 2009, EPA published final designations in the Federal Register announcing those areas that meet or violate the 2006 24-hour $PM_{2.5}$ NAAQS (74 FR 58688). Through that Federal Register notice, EPA formally designated 31 areas including part of Pierce County, Washington, as nonattainment of the 2006 24-hour $PM_{2.5}$ NAAQS, in accordance with the requirements of the federal Clean Air Act Section 107(d). The final designations are effective December 14, 2009, and are based upon 2006 through 2008 monitored $PM_{2.5}$ data.

Figure 1.1 shows an outline of Pierce County's $PM_{2.5}$ nonattainment area, as described in the Federal Register, and the approximate location of the ambient monitoring site used for the designation. The designated 24-hour $PM_{2.5}$ nonattainment area lies approximately 20 miles south of Seattle, Washington, and covers most of metropolitan Tacoma and surrounding communities within Pierce County's Comprehensive Urban Growth Area. There are currently no nonattainment areas for the annual $PM_{2.5}$ NAAQS in Washington State.

As a result of this designation, Washington State (like other affected states) is required to develop a State Implementation Plan (SIP), within three years of the effective date of the final designations, which provides for attainment of the NAAQS as expeditiously as practicable (74 FR 58688). The SIP submission must include an attainment demonstration showing that the application of selected reasonably available control measures and control technologies to specific source types will lead to attainment of the 2006 24-hour $PM_{2.5}$ NAAQS as soon as possible. The exact requirements of the SIP are unknown because EPA has not published implementation instructions for the 2006 $PM_{2.5}$ NAAQS.

Preparation of an effective SIP begins with proper identification and prioritization of emission sources to be controlled. In general, emission sources found to be directly or indirectly contributing to the highest mass concentrations in the nonattainment area should be given priority. Useful information for identifying the most important emission sources to be controlled can be obtained through analysis of speciated $PM_{2.5}$ measurements.

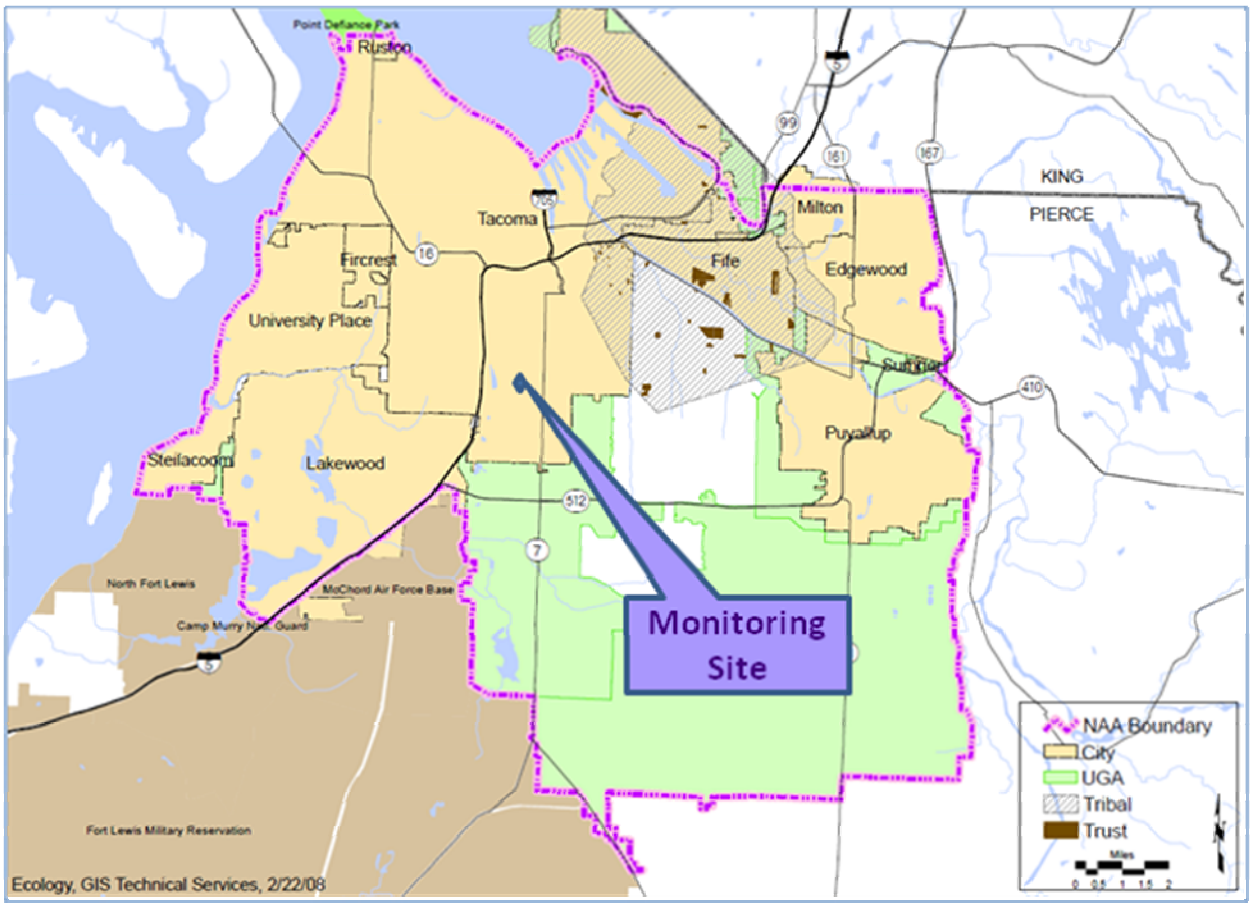


**Figure 1.1. Wapato Hills-Puyallup River Valley Nonattainment Area**. The nonattainment boundary is shown in pink.

In response to the monitored high ambient $PM_{2.5}$ concentrations measured in south Tacoma, and to address nonattainment issues in the region, the Washington State Department of Ecology initiated an effort to identify and quantify the most important sources contributing to the measured mass concentrations within the designated nonattainment area. Existing $PM_{2.5}$ speciation data collected using the Speciation Trends Network (STN) sampling protocols in South Tacoma, Washington, from January, 2006 to May, 2009 were analyzed in this study.

The source apportionment analysis was conducted using Positive Matrix Factorization (PMF; Paatero and Tapper, 1994; Paatero, 1997) and the Conditional Probability Function (CPF; Ashbaugh et al., 1985). Detailed results from this study are presented in the following sections.

# 2.0 EXPERIMENTAL METHODS

## 2.1 Sampling Site and Data Description

The data used in this study were collected between January 11, 2006 and May 7, 2009 at 7802 South L Street in Tacoma, Pierce County, Washington. The sampling site (Latitude 47.1863 $^{o}$, Longitude -122.4515$^{o}$) is operated by Puget Sound Clean Air Agency (PSCAA) and is located approximately 4 miles south of downtown Tacoma. The area surrounding the site is a predominantly low income residential neighborhood. A major north-south freeway (Interstate-5) runs less than one mile west of the site (Figure 2.1). There are also several heavily traveled arterial streets that are located within one mile of the sampling site. An Air Force base (McChord Air Force Base) is located approximately 3 miles southwest of the site, and an Army base (Fort Lewis) is a farther 3 miles southwest. Multiple industries are located in the vicinity of the site, including several major industrial facilities that are located within 6 miles northeast of the sampling site. Major industries located within the Port of Tacoma include a pulp and paper mill; a refuse processing facility; an oil refinery; an agricultural feeds processing facility; and a lime processing plant.

An analysis of emissions inventory data for Pierce County indicates that wood combustion emissions, primarily emissions from wood-fired home-heating devices, are the largest source of emissions in Pierce County. A recent analysis of the area's ambient air quality data further found that the highest total $PM_{2.5}$ mass concentrations in the area are observed exclusively in the winter, with carbonaceous $PM_{2.5}$ being the dominant chemical component on days with the highest $PM_{2.5}$ mass concentration (EPA, 2008b).

Twenty-four-hour $PM_{2.5}$ speciation measurements were made every sixth day according to Speciation Trends Network (STN) protocols. There were a total of 74 species measured, including total $PM_{2.5}$ mass. Ionic species (i.e., ammonium, sulfate, nitrate, sodium, and potassium ions) were analyzed by ion chromatography of material collected on nylon filters in the Andersen RAAS speciation sampler. Other elemental species were measured using energy dispersive x-ray fluorescence of material collected on Teflon® filters in the Andersen RAAS speciation sampler. PSCAA also made concurrent ambient measurements of black carbon using an aethalometer, as well as measurements of multiple meteorological variables.

In this study, species containing at least 75% of concentrations below detection, or missing, were omitted from further analysis. Under this criterion, we omitted the following 24 species (i.e., 32% of all species measured by the STN speciation sampler): antimony (Sb), barium (Ba), cadmium (Cd), cesium (Cs), cerium (Ce), europium (Eu), gallium (Ga), gold (Au), hafnium (Hf), indium (In), iridium (Ir), lanthanum (La), molybdenum (Mo), niobium (Nb), phosphorus (P), samarium (Sm), scandium (Sc), silver (Ag), tantalum (Ta), terbium (Tb), tin (Sn), tungsten (W), yttrium (Y), and zirconium (Zr).


**Figure 2.1. Location of the sampling site with respect to major particle sources.**

We also did not utilize sulfur (S), potassium ion ($K^+$) or sodium (Na) in this study because they were highly correlated with sulfate ($SO_4^{2-}$), potassium (K) and sodium ion ($Na^+$), respectively, suggesting that their ambient concentrations were being double-counted in the data set. Additionally, chromium (Cr), cobalt (Co), mercury (Hg), rubidium (Rb), and selenium (Se) had signal-to-noise ratios of less than or equal to 1.0 (EPA, 2008a) which prevented meaningful statistical fitting of those species. Those species were therefore excluded from further analysis.

The wind speed and direction data used in this study were measured at the same air quality monitoring site described above. The data were downloaded from PSCAA's *TrendGraphing* website: http://trendgraphing.pscleanair.org/. Figure 2.2 shows the area's wind profile during the period, January 11, 2006 through May 7, 2009. It can be observed that most of the wind appeared to be traveling at 1–2 meters per second (m/s), and generally approached from the south-southwest. We observed only three occurrences between January 1, 2006 and May 7, 2009, when the winds exceeded 4 m/s, meaning that winds were generally mild within the study

area. On days when the measured total mass concentrations exceeded 30 µg/m$^3$, winds blew from the southeast approximately two-thirds of the time (Table 2.1), at an average speed of about 0.6 m/s.

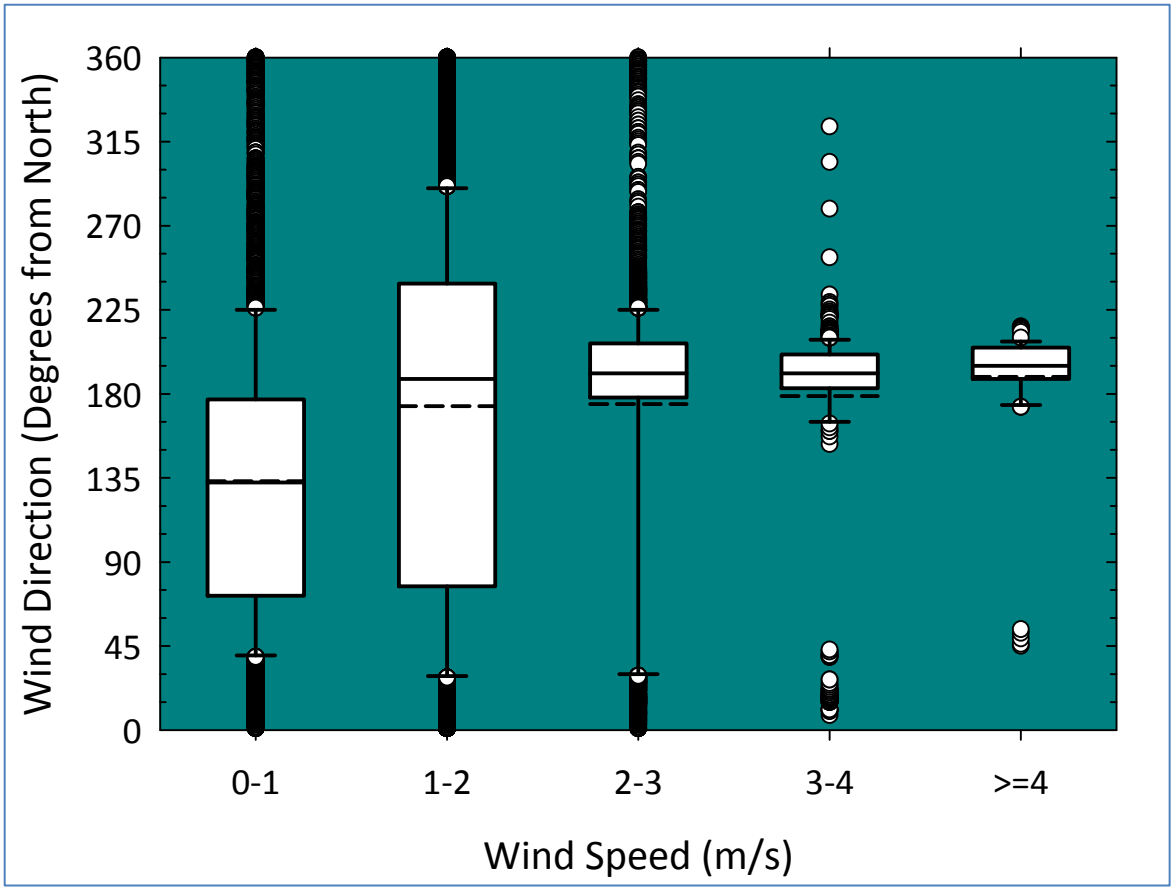


**Figure 2.2. The area's wind profile during the study period**. Plot shows one-hour averaged measurements. Box edges represent the 25$^{th}$ and 75$^{th}$ percentiles of the wind direction. Solid line inside the box is the median wind direction. Dotted line inside the box is the average wind direction. Lower and upper whisker caps are the 10$^{th}$ and 90$^{th}$ percentiles, respectively. Any data outside the 10$^{th}$/90$^{th}$ percentiles are plotted as circular points.

On 5/12/07, STN began using revised thermal optical transmittance and reflectance protocols for organic carbon (OC) and elemental carbon (EC), while the previous protocols were continued up to 7/5/07. In this work, we utilized total EC and total OC data measured using the old thermal optical transmittance (TOT) protocol prior to and including 5/6/07. After 5/6/07, we used total EC and OC data measured by the revised TOT protocol. We did not use thermal optical reflectance (TOR) data because there were no total EC (TOR) data prior to 7/5/07. Also, we did not use data for carbon fractions (i.e., EC1, EC2, EC3, OC1, OC2, OC3, OC4 and OP) because EC fractions were not measured prior to 5/12/07.

**Table 2.1. Total $PM_{2.5}$ mass concentrations and average wind direction on days when the FRM or STN samplers reported ambient mass concentrations exceeding 30 µg/m$^3$**

| Sample Date | FRM Mass Concentration (µg/m$^3$) | STN Mass Concentration (µg/m$^3$) | Average Wind Direction (Degrees) |
|---|---|---|---|
| 2/19/2006 | 33.7 | No data | 107 |
| 11/1/2006 | 32.3 | 33.0 | 119 |
| 12/7/2006 | No data | 32.6 | 209 |
| 12/16/2006 | 68.0 | No data | 79 |
| 12/19/2006 | 32.6 | 32. 7 | 189 |
| 12/28/2006 | 42.7 | No data | 67 |
| 12/31/2006 | 50.2 | 54.3 | 160 |
| 1/12/2007 | 44.7 | 44.9 | 81 |
| 1/15/2007 | 58.6 | No data | 159 |
| 1/27/2007 | 30.8 | No data | 148 |
| 1/30/2007 | 38.2 | 39.1 | 115 |
| 2/2/2007 | 46.7 | No data | 75 |
| 10/27/2007 | 31.7 | 34.5 | 93 |
| 11/8/2007 | 31.5 | 33.2 | 151 |
| 11/23/2007 | 45.3 | No data | 96 |
| 1/24/2008 | 44.2 | No data | 103 |
| 1/25/2008 | 49.7 | No data | 95 |
| 2/18/2008 | 31.7 | 32.8 | 92 |
| 2/21/2008 | 31.1 | No data | 48 |
| 12/5/2008 | 39.2 | No data | 156 |
| 12/23/2008 | 49.2 | No data | 103 |
| 1/19/2009 | 39.3 | 38.3 | 52 |
| 2/3/2009 | 36.8 | No data | 117 |
| 2/18/2009 | 27.0 | 31.1 | 21 |

The average total $PM_{2.5}$ mass concentration measured by the STN speciation sampler was 9.66 µg/m$^3$ (N = 191 samples) while the average total mass concentration measured by the federal reference method (FRM) during this period was 9.62 µg/m$^3$ (N = 394 samples).

**Table 2.2. Summary of data used in this study**.

| Species | Total Number of Valid Samples, N | Percentage of Missing and Below-Detection Values (%)[a] | Statistical Measure (μg/m$^3$)[b] | | | |
|---|---|---|---|---|---|---|
| | | | Average | Standard Deviation | Minimum | Maximum |
| $PM_{2.5}$ Mass | 191 | 2.6 | 9.66 | 8.71 | 0.10 | 54.29 |
| FRM Mass | 394 | 0 | 9.62 | 9.66 | 0.90 | 68.00 |
| Nitrate | 190 | 3.6 | 0.75 | 0.65 | 0.00 | 3.22 |
| Sulfate | 190 | 3.1 | 0.97 | 0.63 | 0.04 | 3.64 |
| Elemental Carbon (EC) | 190 | 1.6 | 0.79 | 1.09 | 0.07 | 7.60 |
| Organic Carbon (OC) | 190 | 2.1 | 3.97 | 4.13 | 0.08 | 28.25 |
| Black Carbon (BC) | 190 | 10.5 | 0.95 | 1.04 | 0.12 | 4.77 |
| Aluminum (Al) | 191 | 37.8 | 0.0199 | 0.0280 | 0.0001 | 0.2390 |
| Ammonium ion ($NH_4^+$) | 190 | 9.2 | 0.38 | 0.34 | 0.01 | 2.24 |
| Arsenic (As) | 191 | 34.7 | 0.0015 | 0.0018 | 0.00001 | 0.0199 |
| Bromine (Br) | 191 | 11.7 | 0.0024 | 0.0020 | 0.00005 | 0.0101 |
| Calcium (Ca) | 191 | 5.1 | 0.0268 | 0.0250 | 0.0006 | 0.1922 |
| Chloride Ion ($Cl^-$) | 191 | 10.2 | 0.14 | 0.25 | 0.001 | 2.34 |
| Chromium (Cr) | 191 | 45.9 | 0.00115 | 0.00126 | 0.00004 | 0.01194 |
| Cobalt (Co) | 191 | 63.3 | 0.00055 | 0.00034 | 0.00006 | 0.00231 |
| Copper (Cu) | 191 | 13.3 | 0.004 | 0.007 | 0.00001 | 0.056 |
| Iron (Fe) | 191 | 2.6 | 0.056 | 0.052 | 0.0002 | 0.336 |
| Lead (Pb) | 191 | 35.2 | 0.00385 | 0.00449 | 0.00005 | 0.03050 |
| Magnesium (Mg) | 191 | 51.0 | 0.015 | 0.022 | 0.0001 | 0.148 |
| Manganese (Mn) | 191 | 21.9 | 0.00215 | 0.00249 | 0.00002 | 0.01567 |
| Mercury (Hg) | 178 | 74.0 | 0.00180 | 0.00117 | 0.00014 | 0.00912 |
| Nickel (Ni) | 191 | 27.0 | 0.0014 | 0.0016 | 0.00001 | 0.0105 |
| Potassium (K) | 191 | 2.6 | 0.10733 | 0.23063 | 0.00142 | 1.69983 |
| Rubidium (Rb) | 191 | 67.3 | 0.00069 | 0.00045 | 0.00001 | 0.00344 |
| Selenium (Se) | 191 | 66.3 | 0.00077 | 0.00045 | 0.000002 | 0.00360 |
| Silicon (Si) | 191 | 4.6 | 0.061 | 0.082 | 0.0003 | 0.715 |
| Sodium Ion ($Na^+$) | 190 | 3.1 | 0.219 | 0.207 | 0.003 | 1.550 |
| Strontium (Sr) | 191 | 57.7 | 0.00160 | 0.00393 | 0.00005 | 0.03968 |
| Titanium (Ti) | 191 | 58.7 | 0.0026 | 0.0031 | 0.0001 | 0.0343 |
| Vanadium (V) | 191 | 36.2 | 0.0029 | 0.0038 | 0.0001 | 0.0306 |
| Zinc (Zn) | 191 | 7.7 | 0.0100 | 0.0109 | 0.0002 | 0.0581 |

[a]In the original data set after blank correction.

[b]After treatment for missing and below-detection values.

A comparison of the measured concentrations by these two methods for the days when the FRM monitor predicted ambient concentrations greater than 30 $\mu g/m^3$ (Table 2.1) indicates that the STN speciation sampler closely replicated the FRM's values. In fact, the mass concentrations obtained by the STN sampler tended to be slightly higher than the corresponding FRM values. Note that STN data were obtained every sixth day, compared to an every-third-day frequency for the FRM mass measurements. Overall, on those days when both the STN and FRM samplers recorded a $PM_{2.5}$ mass measurement, the two measurements were strongly correlated, with an overall correlation coefficient ($r^2$) of 0.95 (N = 186 samples).

Except for organic carbon, all of the speciation data used in this study were blank-corrected using the provided field blanks. For organic carbon (OC), we corrected for OC sampling artifacts by plotting the uncorrected total OC against the measured total $PM_{2.5}$ mass and using the y-intercept as the correction. No OC field blanks were subtracted from the raw concentrations as it was assumed that the artifacts encompassed the field blank.

We did not exclude data associated with fireworks primarily because, as shown in Table 2.1, both the STN and FRM monitors reported unusually high concentrations on one of the suspected fireworks days. Suspected fireworks days were 7/4/2006, 12/31/2006, 7/5/2007, 7/5/2008 and 1/1/2009. Since the high total mass concentration on 12/31/2006 may have affected the $PM_{2.5}$ design value for that year, we therefore found it important to ascertain the exact contribution of fireworks to the measured ambient concentrations in the area.

Table 2.2 provides a statistical summary of the final species used in the source apportionment analysis. For completeness and data comparison, Table 2.2 also shows the statistics for total $PM_{2.5}$ mass as measured by the FRM sampler. Because the average measured mass concentrations determined by STN and FRM methods are in very good agreement (9.66 and 9.62 $\mu g/m^3$, respectively), it is safe to conclude that, the average source contributions resolved in this study would not be expected to substantially change if the analysis relied exclusively on FRM measurements.

## 2.2 Model Description

We utilized two primary data analysis methods in this analysis: Positive Matrix Factorization (PMF) and the Conditional Probability Function (CPF). Both of these methods have been extensively utilized and discussed in the air quality management literature. For completeness, the two methods are summarized below.

### 2.2.1 Positive Matrix Factorization (PMF)

PMF is a mathematical (statistical) technique that decomposes a matrix of speciated ambient sample data into a source contributions matrix and a source profile matrix. The PMF method has been discussed in detail by EPA (2008a). The latest version of EPA's formulation of the PMF model (EPA PMF 3.0) was used in this study. The PMF algorithm attempts to find a mathematical solution that satisfies several mass apportionment conditions (Hopke et al., 1980; Paatero, 1997). In general, the model attempts to estimate the optimum number of independent sources (or "factors") that adequately explain the observations at the sampling site. The resolved

sources are identified and validated through information known *a priori* about the airshed being studied. The modeling procedures recommended by EPA (2008a) were followed in this study.

#### 2.2.1.1 Data Treatment for PMF Analysis

A PMF analysis requires extensive pre-treatment of data before the data can be used with the model. The data set must not contain missing, zero or non-positive concentrations. Negative or zero concentrations that typically result from blank corrections must be appropriately substituted with non-negative values. Any missing concentrations in a valid sample must be estimated prior to application of the model. Finally, each reported concentration must be accompanied by an uncertainty value that represents the sum of all uncertainties associated with that measurement.

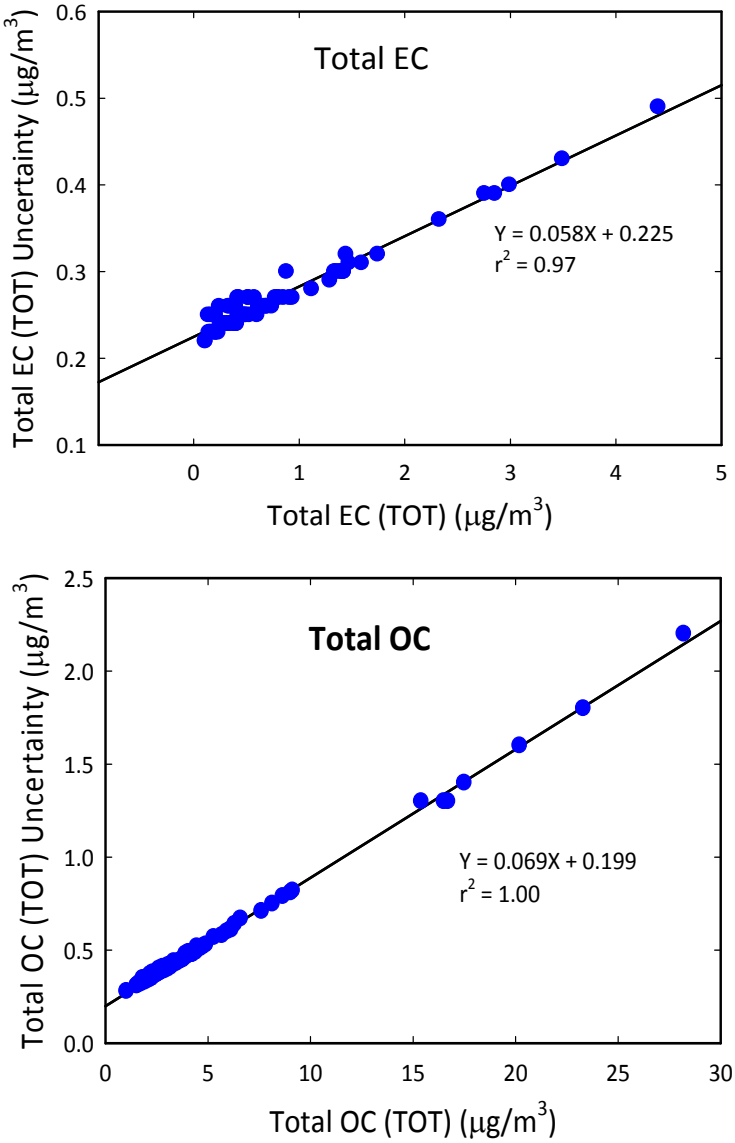


**Figure 2.3. Plots of measured uncertainties (y-axis) against measured concentrations (x-axis) for elemental carbon (EC) and organic carbon (OC).**

In this study, missing data were replaced with interpolated concentrations from the closest given values or estimated non-negative values. For such data points, the uncertainty was calculated as four times the estimated concentration. Except for aluminum (Al), values reported to be below detection were replaced with one-half of the sample detection limit for that species. We then calculated the associated uncertainties for such data points as twice the estimated concentration. In accordance with the air quality monitoring advisory for Al (<http://vista.cira.colostate.edu/improve/Data/QA_QC/Advisory/da0010/da0010_Almdl.pdf>), if Al was reported below the detection limit, we calculated the associated concentration data point as one-third of the silicon (Si) concentration value for that sample, based on the approximate ratio of Al to Si on days when valid Al and Si values were reported. The corresponding uncertainties were calculated as four times the estimated concentrations.

For OC and EC, since no measurement uncertainties were reported under the revised TOT or TOR protocols, the required measurement uncertainties were estimated by regressing the reported uncertainties against the ambient concentrations determined under the old TOT and TOR protocols. Based on the regression analysis, the required uncertainties were calculated using the following equations:

$$\text{For EC:} \quad \text{EC Unc}_{ij} = (0.058)\times(\text{EC Conc}_{ij}) + 0.225 \qquad (1)$$

$$\text{For OC:} \quad \text{OC Unc}_{ij} = (0.069)\times(\text{OC Conc}_{ij}) + 0.199 \qquad (2)$$

where $\text{Unc}_{ij}$ is the calculated (estimated) measurement error for species j and sample i; $\text{Conc}_{ij}$ is the observed species concentration; and the constants are regression coefficients (Figure 2.3).

Because no measurement uncertainties were provided for black carbon (BC), the required uncertainties were calculated using the equation reported by Ogulei et al. (2006), with the arbitrary constant set to 0.1. An empirical extra modeling uncertainty of 20% was added to the estimated uncertainties of all species to account for uncorrected random and systematic errors. In addition, $PM_{2.5}$ mass concentrations were down-weighted by a factor of 3 in the PMF analysis in order to minimize their effect on the apportionment of other species.

#### 2.2.1.2 Optimum Number of Sources

As recommended by EPA (2008a), the optimum number of sources was based primarily upon the quality of the least-squares fit and the interpretability of the model results. The experimental residual sum of squares, Q, should be approximately equal to its theoretical value (EPA, 2008a). The theoretical value of Q was approximated by the total number of data points minus the total number of degrees of freedom, that is,

$$Q_{\text{theoretical}} = (\text{number of species} \times \text{number of samples}) - (\text{number of species} \times \text{number of sources}) - (\text{number of samples} \times \text{number of species}) \qquad (3)$$

### 2.2.2 The Conditional Probability Function (CPF)

The CPF is a probabilistic tool that estimates the probable direction associated with ambient concentrations that exceed an operationally-defined threshold. In this study, the threshold was defined as the highest 25% (i.e., 75$^{th}$ percentile) of the resolved contributions. We calculated the CPF for each wind sector using the following equation:

$$CPF_{\Delta\theta} = \frac{m_{\Delta\theta}}{n_{\Delta\theta}} \qquad (4)$$

where $\Delta\theta$ is the wind sector (20$^o$ each); $m_{\Delta\theta}$ is the number of contribution occurrences from wind sector $\Delta\theta$ in which the resolved contributions fell in the upper 25% of all contributions; and $n_{\Delta\theta}$ is the total number of contribution occurrences from wind sector $\Delta\theta$.

For the purpose of calculating the CPF, data points corresponding to wind speeds below 1 m/s (2.2 miles per hour) were initially excluded in the preliminary analysis. This is because winds slower than 1 m/s tend to lead to wind meandering around the sampling site, which typically makes it difficult to identify potential point source locations. However, because previous studies found that exceedances of the 24-hour $PM_{2.5}$ national ambient standard typically occurred at very low wind speeds, the final analysis was refined to include all wind speeds in the CPF calculations. The CPFs presented in this report therefore include all measured 24-hour averaged wind speeds in the calculations.

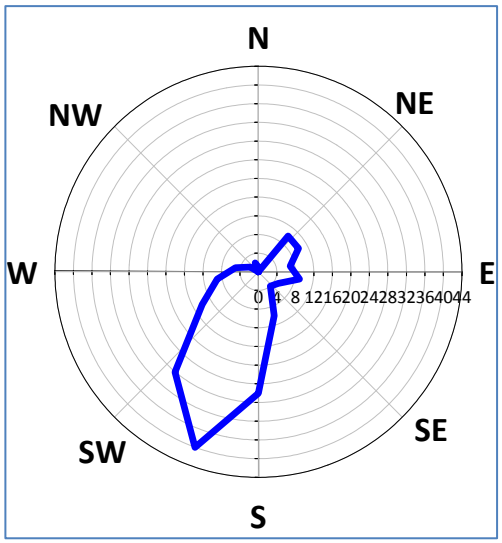


**Figure 2.4. Overall wind profile.** Numbers in the plot indicate number of occurrences from a given wind sector.

A plot of the overall wind profile is shown in Figure 2.4. A comparison between Figures 2.2 and 2.4 indicates that the two profiles both show that the predominant wind direction was south-southwest. This is particularly relevant if there are significant sources located to the south-southwest direction relative to the sampling site.

We also calculated CPFs for individual species to determine the directions associated with high measured concentrations for those species (CPFs not shown here). Those CPFs showed similar potential source locations associated with the measured organic carbon (OC) and black carbon (BC) concentrations. There were also similarities between potential source locations associated with the measured nickel (Ni) and vanadium (V) concentrations. Total $PM_{2.5}$ mass emissions appeared to come from multiple directions as did emissions of most species.

# 3.0 SOURCE APPORTIONMENT RESULTS

## 3.1 Criteria for Source Identification

In this study, we defined the "correct" solution as the optimum number of sources that corresponded to acceptable least squares and regression statistics, and physically interpretable source profiles. The solution was checked for stability through a bootstrapping technique. Bootstrapping is a re-sampling technique in which a new data set having the same dimensions as the original data set is randomly generated (sampled) from the original data set and analyzed. The resulting source profiles and contributions are compared with the original (base) solution (EPA, 2008a).

We successfully resolved and identified eleven sources based upon the following criteria:

1) *The elemental composition of the source profile*. The presence of specific source signatures in a resolved source profile generally permitted the identification of that source profile. The resolved source profiles were compared with profiles available through the EPA's SPECIATE database.

2) *The seasonal behavior of the source contributions*. This enabled distinction between sources that are known to peak during the summer from those that typically peak in the winter. For example, secondary nitrate and wood smoke could be distinguished from secondary sulfate based on this criterion.

3) *The wind direction(s) corresponding to the highest source contributions*. Through the CPF analysis, we were able to identify the potential locations of point sources because resolved concentrations almost always peaked when winds blew from the direction of those sources.

4) *The resolved source contributions versus the emissions inventory*. Knowledge of the area's emissions inventory and published information on source contributions enabled identification of certain sources, such as wood smoke.

We identified the eleven emission sources as: wood smoke, gasoline vehicles, diesel vehicles, fugitive dust, fireworks, secondary nitrate, secondary sulfate, oil combustion and ships, arsenic-rich industrial emissions, freshly-emitted sea salt, and processed ("aged") sea salt. On average, the eleven sources accounted for 93% of the measured $PM_{2.5}$ mass. The remaining 7% may represent the effect of noise in the measured data and the apportionment itself, other relatively insignificant sources or a combination of these factors.

## 3.2 Overall Contributions

Table 3.1 shows the average contributions in micrograms per cubic meter ($\mu g/m^3$) resolved in this analysis. The contributions have been averaged over the entire sampling period. The percentage contributions are shown in Figure 3.1. Overall, wood smoke was the dominant source during the study period with an average contribution of 4.0 $\mu g/m^3$, or about 45% of the total apportioned $PM_{2.5}$ mass. Additionally, PMF resolved significant contributions from secondary aerosol (25%) and motor vehicles (13%). A break-down of the source contributions among the various seasons is provided later in the report.

**Table 3.1. Average contributions resolved by the PMF model.**

| Resolved Source | Average Contribution ($\mu g/m^3$) | Standard Deviation ($\mu g/m^3$) |
|---|---|---|
| Wood Smoke | 4.0 | 4.9 |
| Secondary Nitrate | 1.2 | 1.4 |
| Secondary Sulfate | 1.0 | 0.9 |
| Gasoline Vehicles | 0.9 | 1.3 |
| Arsenic-rich Industrial Emissions | 0.5 | 0.6 |
| Fugitive Dust | 0.4 | 0.5 |
| Fresh Sea Salt | 0.3 | 0.6 |
| Diesel Vehicles | 0.3 | 0.3 |
| Fireworks | 0.2 | 0.7 |
| Oil Combustion and Ships | 0.1 | 0.2 |
| Aged Sea Salt | 0.03 | 0.02 |

## 3.3 Seasonal Contributions

To better understand the contributions of individual sources, we divided the sampling period into four seasons as follows: "Winter", which was used to represent the calendar months of December, January and February; "Spring", which represented March, April and May; "Summer" for June, July and August; and "Fall" for September, October and November. To better resolve the contribution of wood smoke in the study area, we also defined a "heating" season (October through March) and a "non-heating" season (April through September). Boundaries for the heating and non-heating seasons were based on existing data on wood stove use within the Puget Sound area. The heating season was defined to account for those months when ambient temperatures were low enough that home heating was expected to be prevalent.

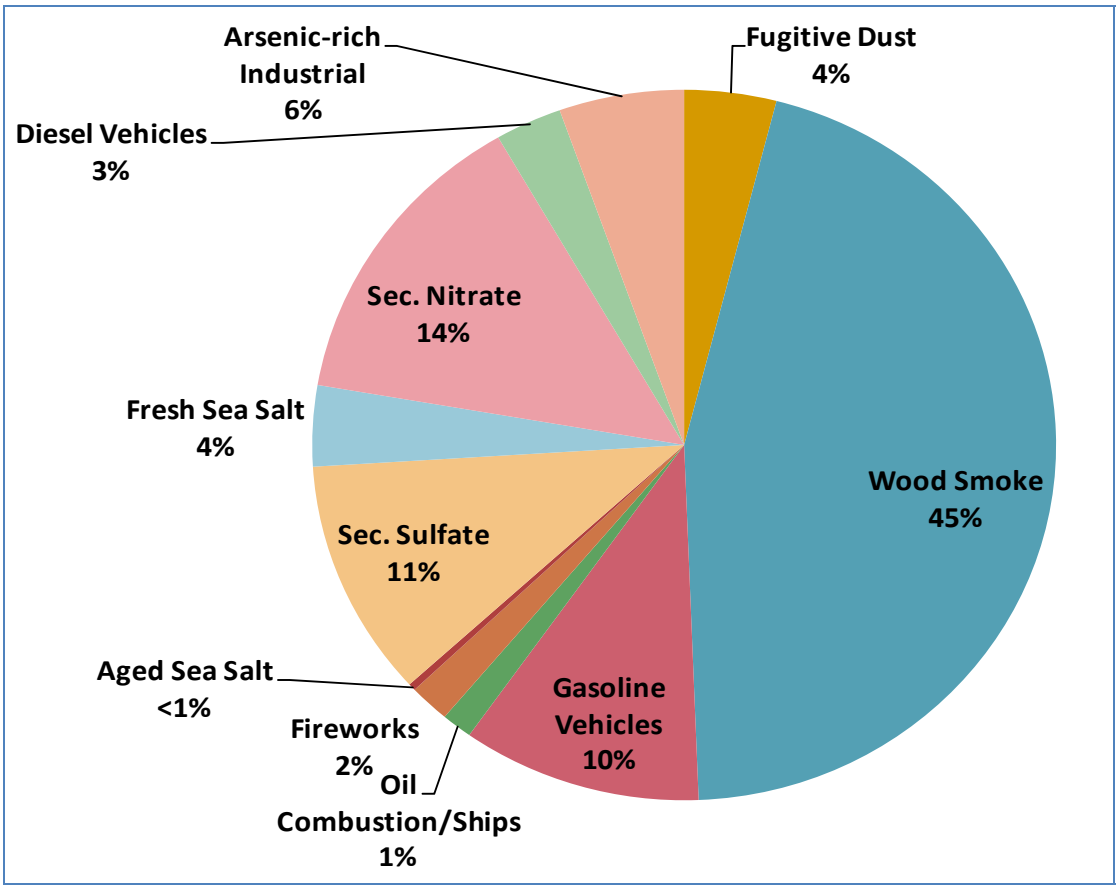


**Figure 3.1. Percentage contributions, averaged over the entire modeling period.**

Figure 3.2 shows the resolved average contributions by season. It can be observed that strong seasonality was observed in some, but not all, of the resolved sources. Specifically, wood smoke, fireworks, secondary nitrate, motor vehicles, industrial emissions, and fresh sea salt exhibited pronounced fluctuations in average contributions between two or more seasons. Most of the fugitive dust and fireworks contributions occurred in the summer, while most of the wood smoke contributions occurred in the winter.

Average contributions from motor vehicles and industry were highest in the winter probably due to the low atmospheric mixing height in the winter. Also, for motor vehicles, the increased number of cold-starts in the winter may have contributed to increased motor vehicle emissions in the winter.

The differences in contributions between heating and non-heating months can be seen in Figure 3.3. The most noticeable change in average contributions between heating and non-heating seasons was observed with wood smoke. As discussed later in the report, this observation is not surprising given the reported heavy reliance of the study area's local residents on wood heating as the primary source of heat in the winter.

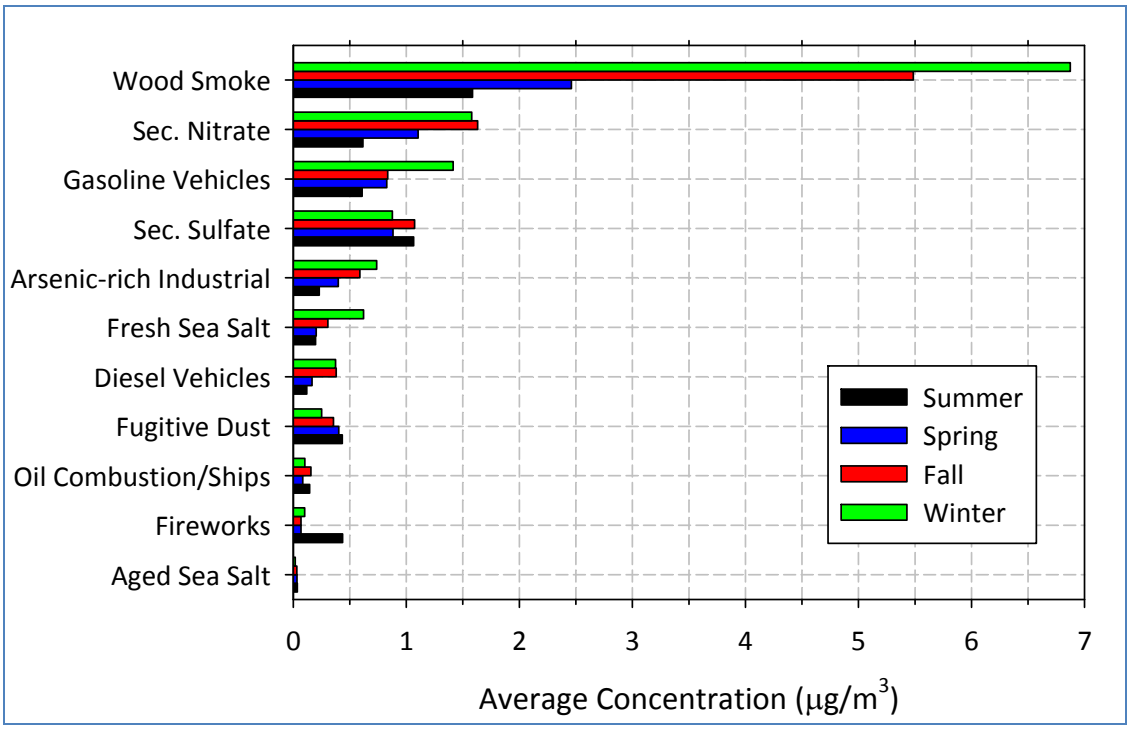


**Figure 3.2. Average contributions by season**. The majority of wood smoke contributions originated in the winter and fall, while most of the fireworks contributions were observed in the summer months.

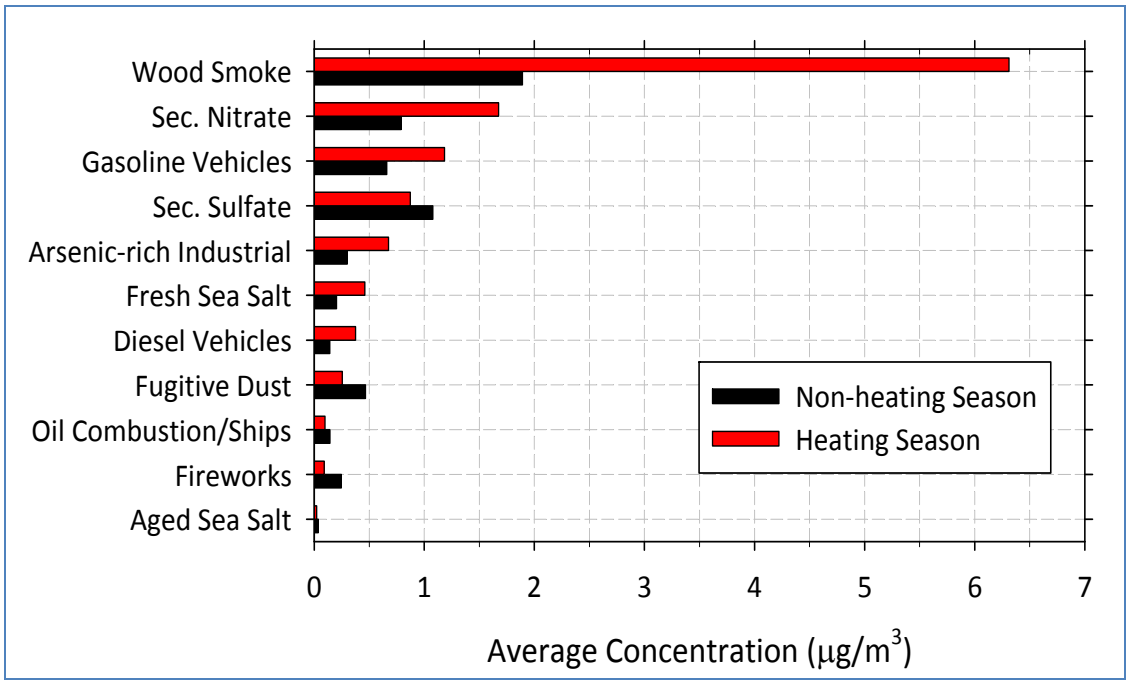


**Figure 3.3. Heating vs. non-heating contributions**. The most significant change in average contributions was observed with wood smoke.

## 3.4 Weekday and Weekend Contributions

Differences between weekday and weekend average concentrations were generally less pronounced than seasonal average contributions. As shown in Figure 3.4, the observed differences between weekday and weekend concentrations for some of the sources were within experimental error suggesting that daily human activities were not the exclusive explanation for the observed contributions from those sources. In fact, this analysis found that weather conditions also played a significant role in the observed $PM_{2.5}$ concentrations on certain days.

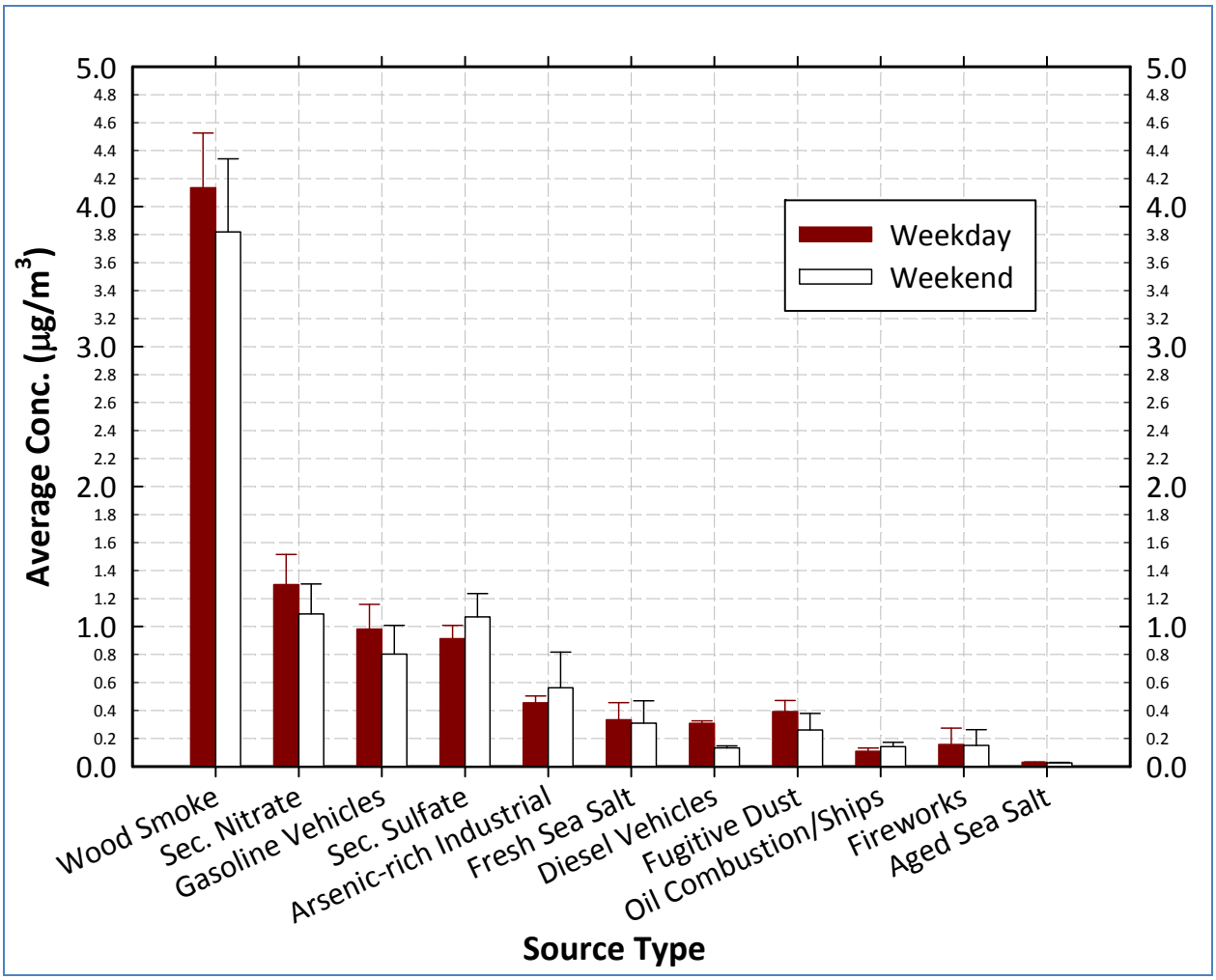


**Figure 3.4. Weekday/weekend variation**. Weekday refers to Monday through Friday; Weekend is Saturday and Sunday. Error bars are standard deviations of the mean.

Weekday contributions were noticeably higher than weekend average contributions for motor vehicles, secondary nitrate and fugitive dust. Weekend average contributions were higher than weekday values for secondary sulfate, industrial emissions and oil combustion/ships. The weekday-weekend difference was within experimental error for the other sources, including wood smoke.

## 3.5 Annual Contributions

Table 3.2 shows annual average contributions for the years used in this study. Although the data available for 2009 represented less than half of the year (January 11, 2006 through May 7, 2009), it is possible to notice that average contributions for wood smoke and industry appeared to annually decrease from the 2006 levels. This annual decline appeared to exist in absolute terms (concentrations) and relative terms (percentage). There was no indication of a decline in annual average contributions from other source categories.

Note that while there is a noticeable decline in the annual averaged wood smoke emissions, a longer time period is needed to establish a trend in contributions. Moreover, the 98$^{th}$ percentile values of the 24-hour concentrations did not show a similar decline. The 98$^{th}$ percentile concentrations for wood smoke were 23, 24 and 13 μg/m$^3$ for 2006, 2007 and 2008, respectively, while the 98$^{th}$ percentile concentrations for motor vehicles were 2.3, 1.9 and 1.2 μg/m$^3$ for 2006, 2007 and 2008, respectively.

**Table 3.2. Source contributions averaged over individual years.**

| Sample Year | 2006 | 2007 | 2008 | 2009* |
|---|---|---|---|---|
| Measured $PM_{2.5}$ Mass (μg/m$^3$) | 9.4 | 10.8 | 8.3 | 10.4 |
| **Average Concentrations (μg/m$^3$) (Percentage of Measured Mass)** | | | | |
| Wood Smoke | 4.8 (51%) | 4.4 (41%) | 3.0 (37%) | 3.7 (35%) |
| Secondary Aerosol | 2.0 (21%) | 2.5 (23%) | 2.1 (25%) | 2.4 (23%) |
| Motor Vehicles | 0.9 (9%) | 1.2 (11%) | 1.0 (11%) | 2.7 (26%) |
| Industry | 0.6 (6%) | 0.6 (5%) | 0.3 (4%) | 0.5 (5%) |
| Other Identified Sources | 1.1 (12%) | 0.8 (8%) | 1.1 (13%) | 0.7 (7%) |

* Only measurements made until May 7, 2009 were available for analysis. Therefore, caution should be exercised in interpreting the 2009 figures.

## 3.6 Contributions on Days When the Measured Total Mass Concentration Was Elevated

Figure 3.5 shows the range of percentage contributions for four different ambient $PM_{2.5}$ mass concentrations. The resolved average contributions on days when the measured total $PM_{2.5}$ mass concentration was or exceeded 30 μg/m$^3$ are shown in Table 3.3. As indicated by Figure 3.5 and Table 3.3, wood smoke was responsible for at least one-half of the observed total mass on most days when the measured total $PM_{2.5}$ mass concentration exceeded 30 μg/m$^3$. On those days when the measured total $PM_{2.5}$ mass concentration was or exceeded 30 μg/m$^3$, the wood smoke proportion reached 72% at one time, on 11/1/2006. The corresponding total mass concentration

was 33 µg/m$^3$. Table 2.1 (Section 2.1) indicates that the average wind direction on that day (11/1/2006) was southeast.

Wood smoke contributions also averaged about 52% when the total $PM_{2.5}$ mass concentration exceeded 20 µg/m$^3$, which is a healthy air goal established by the Washington State Department of Ecology (Figure 3.5). On two occasions when the total $PM_{2.5}$ mass concentration exceeded 20 µg/m$^3$ during the study period, the wood smoke contribution was 72% of the daily total mass.

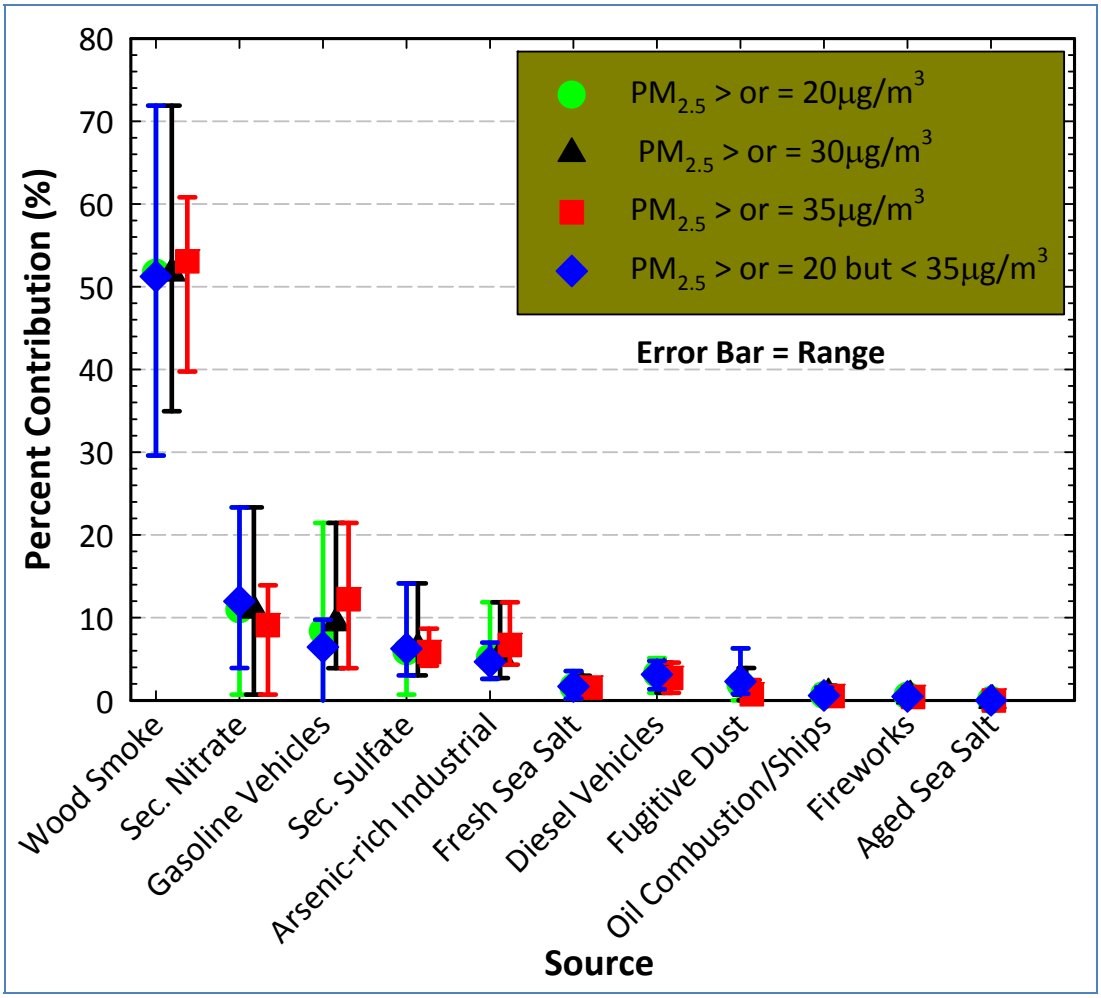


**Figure 3.5. Percentage contributions on days when the measured total $PM_{2.5}$ mass concentration was elevated**. For completeness, four concentration ranges were evaluated: ≥ 20 µg/m$^3$ (circular symbols); ≥ 30 µg/m$^3$ (triangles); ≥ 35 µg/m$^3$ (squares); and 20 ≤ $PM_{2.5}$ <35 µg/m$^3$ (diamonds). Error bars represent the data range.

Generally, on elevated days (i.e., days with measured $PM_{2.5}$ mass ≥ 30 µg/m$^3$) where the resolved wood smoke contribution exceeded 50%, daily-averaged winds blew from the southeast or southwest approximately 70% of the time. This suggests that wood smoke sources located to the southeast and southwest of the sampling site may have been responsible for the majority of the observed wood smoke concentrations on those days.

Besides wood smoke, motor vehicles and secondary aerosol (secondary nitrate plus secondary sulfate) also contributed significant amounts to the measured total mass on most days when the $PM_{2.5}$ ambient concentration was or exceeded 30 $\mu g/m^3$. Motor vehicles contributed about one-quarter of the total measured mass on Martin Luther King Jr. Day (1/19/2009). An analysis of the measured $PM_{2.5}$ data showed that there was a marked increase in ambient concentrations of multiple species on that day. The total $PM_{2.5}$ mass was 38 and 39 $\mu g/m^3$ according to the STN and FRM samplers, respectively. The average wind speed on 1/19/2009 was relatively mild at 0.5 m/s (1.1 miles per hour) approaching from the east. Motor vehicle contributions were also significant on 12/31/2006 when the measured total mass concentration was the highest (54 $\mu g/m^3$).

Secondary aerosol (secondary nitrate plus secondary sulfate) was responsible for about one-third of the total mass on 11/8/2007, and about one-fifth of the total mass on several other days, including 1/30/2007, 10/27/2007, 2/18/2008 and Martin Luther King Jr. Day (1/19/2009). These contributions are significant, and may suggest a relationship between the resolved secondary aerosol, wood smoke and motor vehicles on the days with elevated ambient $PM_{2.5}$ mass concentrations. However, further analysis is needed to better characterize the sources of secondary aerosol within the study area.

**Table 3.3. Contributions on days when the observed $PM_{2.5}$ mass concentration was greater than or equal to 30 $\mu g/m^3$.**

| Sample Date | Measured $PM_{2.5}$ Mass ($\mu g/m^3$) | Wood Smoke | Secondary Aerosol | Motor Vehicles | Industry | Other Identified Sources |
|---|---|---|---|---|---|---|
| 11/1/2006 | 33.0 | 72% | 8% | 10% | 7% | 4% |
| 12/7/2006 | 32.6 | 51% | 13% | 12% | 7% | 5% |
| 12/19/2006 | 32.7 | 63% | 12% | 9% | 5% | 3% |
| 12/31/2006 | 54.3 | 53% | 5% | 16% | 12% | 4% |
| 1/12/2007 | 44.9 | 59% | 17% | 6% | 4% | 2% |
| 1/30/2007 | 39.1 | 61% | 20% | 12% | 6% | 4% |
| 10/27/2007 | 34.5 | 52% | 21% | 9% | 6% | 3% |
| 11/8/2007 | 33.2 | 35% | 37% | 11% | 3% | 6% |
| 2/18/2008 | 32.8 | 37% | 23% | 12% | 3% | 9% |
| 1/19/2009 | 38.3 | 40% | 18% | 26% | 5% | 3% |
| 2/18/2009 | 31.1 | 46% | 15% | 16% | 3% | 5% |

# 4.0 DETAILED RESULTS AND DISCUSSION

The PMF results presented in Section 3.0 indicate that the airshed in south Tacoma is dominated by wood smoke and a select number of sources. The effects of individual sources on the measured ambient mass concentrations were typically exacerbated by air stagnation events. For example, there appeared to be an air stagnation event on 12/31/2006, corresponding to an average wind speed of about 1 mile per hour (0.4 m/s) blowing from the south-southeast. The observed 24-hour ambient $PM_{2.5}$ concentration on this day was 54 $\mu g/m^3$. Because a significant number of wood smoke sources were located to the southeast of the sampling site, the effect of those sources may have been exacerbated by stagnation and inversion events on 12/31/2006. Similarly, the effect of fireworks on 12/31/2006 may have been more significant than had there been no stagnation or meteorological inversion on that day.

In a previous analysis, the fastest winds from the south-southwest quadrant were found to correspond to the lowest $PM_{2.5}$ mass concentrations while the slowest winds from the east to southeast corresponded to the highest $PM_{2.5}$ concentrations (EPA, 2008b). This illustrates that stagnations and inversions, such as those typically prevalent in Tacoma in the winter and fall, are additionally responsible for the area's elevated $PM_{2.5}$ mass concentrations in the winter and fall.

## 4.1 Wood Smoke Contributions

As presented in Section 3.0, wood smoke accounted for about 45% of the overall average mass. The maximum wood smoke contribution on any signal day was 72% of the daily $PM_{2.5}$ mass concentration. The maximum wood smoke contribution (72%) was observed on two occasions: 11/1/2006 and 12/8/2007, when the measured daily $PM_{2.5}$ mass concentrations were 33 and 21 $\mu g/m^3$, respectively. This analysis was not able to distinguish between the various types of wood smoke sources. However, based on emissions inventory and census information collected by Ecology and PSCAA, we believe that the wood smoke contributions resolved in this analysis represent combined contributions from wood stoves and other wood-fired home heating devices. Significant contributions from outdoor burning are not expected because the area surrounding the sampling site is classified as an Urban Growth Area (UGA) where outdoor burning is prohibited.

Figure 4.1 shows a plot of the predicted source profile for wood smoke emissions. Wood smoke emissions were characterized by high abundances of organic carbon (OC), elemental carbon (EC), black carbon (BC) and potassium (K). About 80% of OC, 60% of BC, 50% of EC and 40% of K were apportioned to wood smoke. All of these species are important markers for wood smoke and their relative abundances are consistent with abundances reported in the source apportionment literature (e.g., Kim and Hopke, 2008a). The wood smoke concentrations correlated very well with BC ($r^2 = 0.89$), total OC ($r^2 = 0.97$), total EC ($r^2 = 0.79$) and total $PM_{2.5}$ mass concentrations ($r^2 = 0.92$).

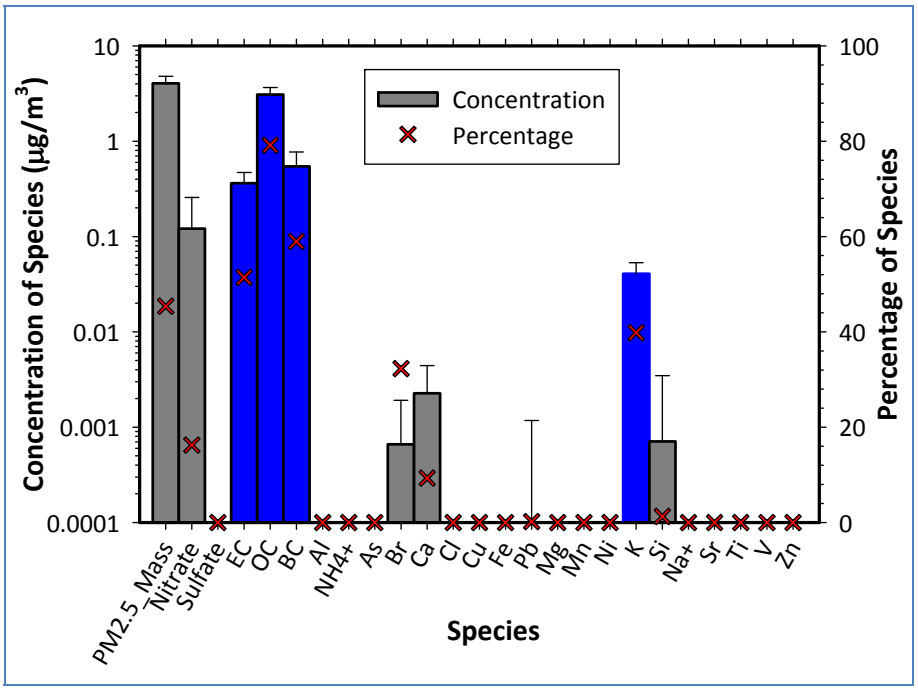


**Figure 4.1. Wood smoke source profile.** "Percentage" refers to the percentage of that species which was apportioned to a specific source. Error bars are standard deviations of the bootstrapping factors. Signature species are shown with blue bars.

The wood smoke contributions resolved by this analysis differ somewhat with contributions observed in neighboring Seattle, Washington. Seattle area studies have typically reported lower wood smoke contributions. For example, Maykut et al. (2003), Wu et al. (2007), and Kim and Hopke (2008a) reported contributions of 7-37% in various areas near Seattle. Kim and Hopke (2008a) reported a significant difference in wood smoke contributions between the residential and downtown areas of Seattle. In their study, wood smoke accounted for about 31% of the apportioned mass in Lake Forest Park (residential) and 7-10% in the commercial sites (Olive St., Beacon Hill, Duwamish).

Conversely, comparable average wood smoke contributions to this study have been reported from Spokane, WA (44%) and Pullman, WA (38%) by Kim et al. (2003) and Jimenez et al. (2006), respectively. A previous source apportionment study, designed for use in defining the extent of the Tacoma area nonattainment boundary, estimated that wood smoke accounted for as much as 60-90% of the measured $PM_{2.5}$ mass when the measured total mass exceeded 30 $\mu g/m^3$ (EPA, 2008b).

The CPF for wood smoke is shown in Figure 4.2. The CPF shows that the predominant sources of wood smoke are located approximately to the south and

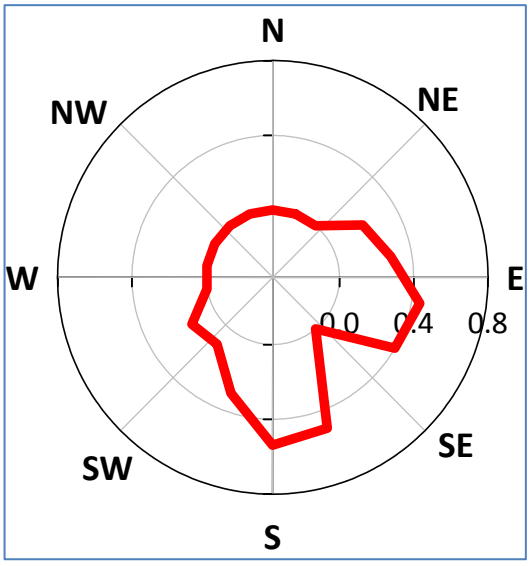


**Figure 4.2. CPF for wood smoke.**

southeast of the sampling site. This is consistent with suspected locations of residences that rely on wood stoves for residential heating (Figure 4.3).

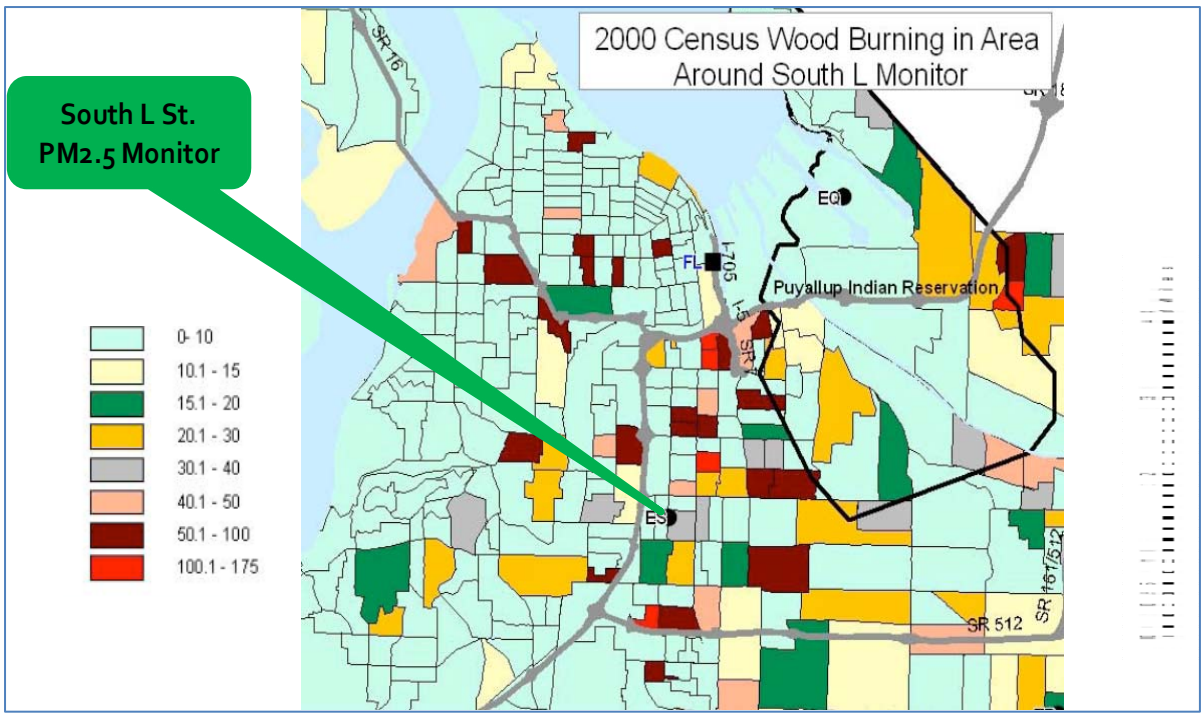


**Figure 4.3. Number of homes using wood as a primary heating source per square mile, in the Tacoma area (Onstad and Simpson, 2008)**. Note that this map reports 2000 census information, which may no longer be representative of current practice. The map also doesn't include the many people who use wood for secondary heat and ambience, which may lead to an underestimate of actual wood stove use in the area.

The CPF also indicates contributions from the southwest, which is also the direction of the overall wind profile (Figure 2.4). This may suggest that the wind direction was also a factor in the observed contributions at the receptor meaning that any wood smoke sources located to the southwest of the sampling site had an influence on the $PM_{2.5}$ mass concentrations recorded at the sampling site. However, as stated above, wood smoke sources located to the south and southeast of the receptor were the most significant.

Figure 4.4 shows the time series of wood smoke alongside the time series for total OC determined by the STN sampling protocol, BC determined by the aethalometer, and total mass measured by the federal reference method. In most cases, total $PM_{2.5}$ mass peaked if wood smoke peaked suggesting that wood smoke likely caused the observed exceedances of the ambient standard on certain days.

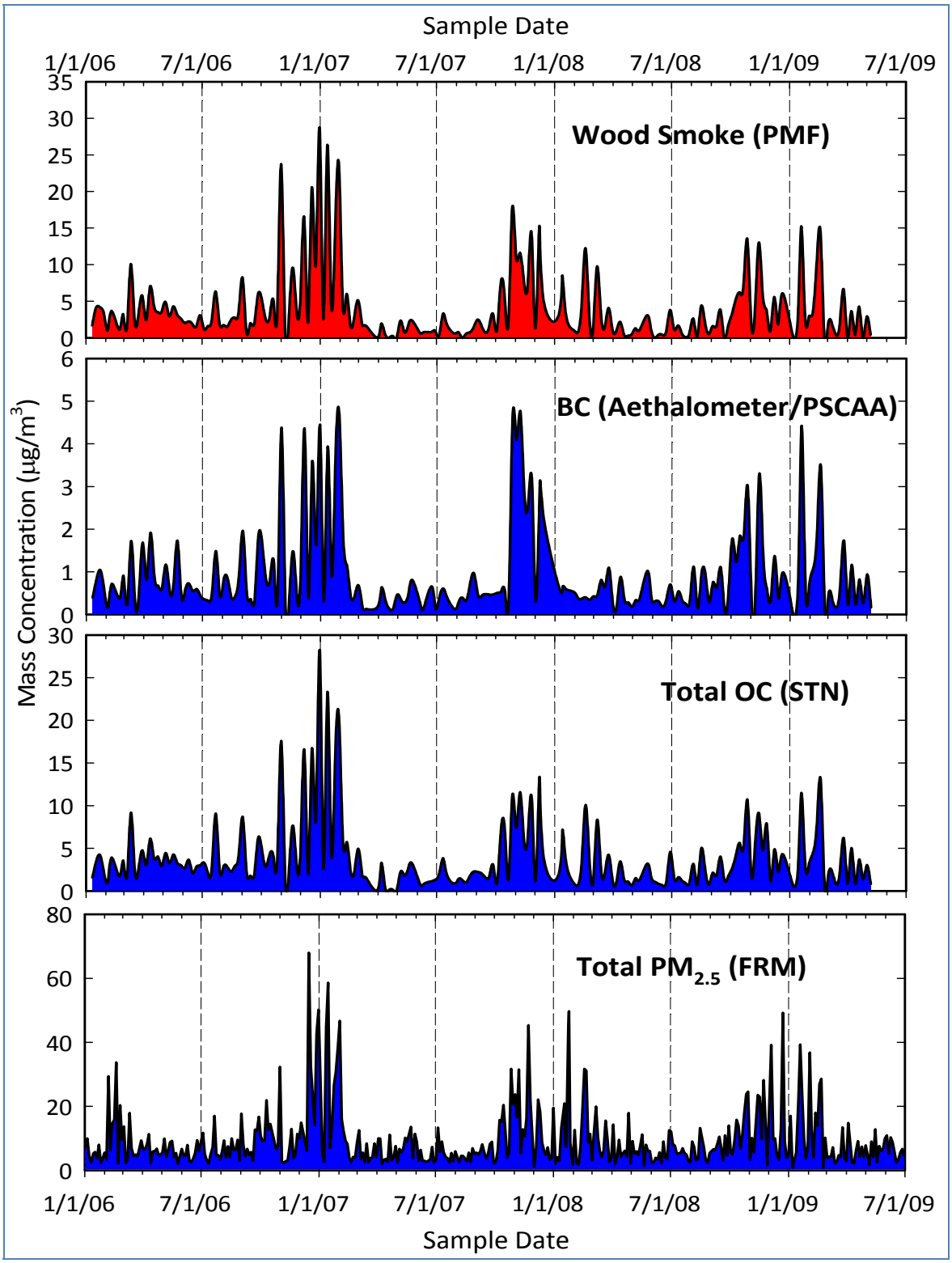


**Figure 4.4. Wood smoke, BC, OC, and $PM_{2.5}$ time series.** Only the FRM mass series is shown because the FRM and STN mass series were identical. Wood smoke was highly correlated with OC, BC and total mass. The correlation with elemental carbon (EC) was also strong. Note the difference in vertical scales.

## 4.2 Motor Vehicles (Gasoline and Diesel)

We resolved two profiles for motor vehicles, accounting for about 13% of the total apportioned mass, averaged over the entire sampling period. The two profiles represented emissions from gasoline-fired and diesel-fired vehicles. While this analysis did not utilize carbon fractions to aid in the separation of gasoline and diesel contributions, it was possible to recognize the difference between the two profiles based upon their total OC and EC relative abundances as well as the existence or non-existence of certain brake-wear metals and fuel oil additives.

Figures 4.5(a) and 4.5(b) show profiles for gasoline and diesel vehicles, respectively. The observed pollutant loadings are similar to loadings reported in gasoline and diesel vehicle emission inventories and other source apportionment studies. For example, the high proportions of manganese (Mn) and iron (Fe) apportioned to the diesel profile are consistent with reported findings from the Seattle area (Maykut et al., 2003) and Phoenix (Ramadan et al., 2000; Lewis et al., 2003).

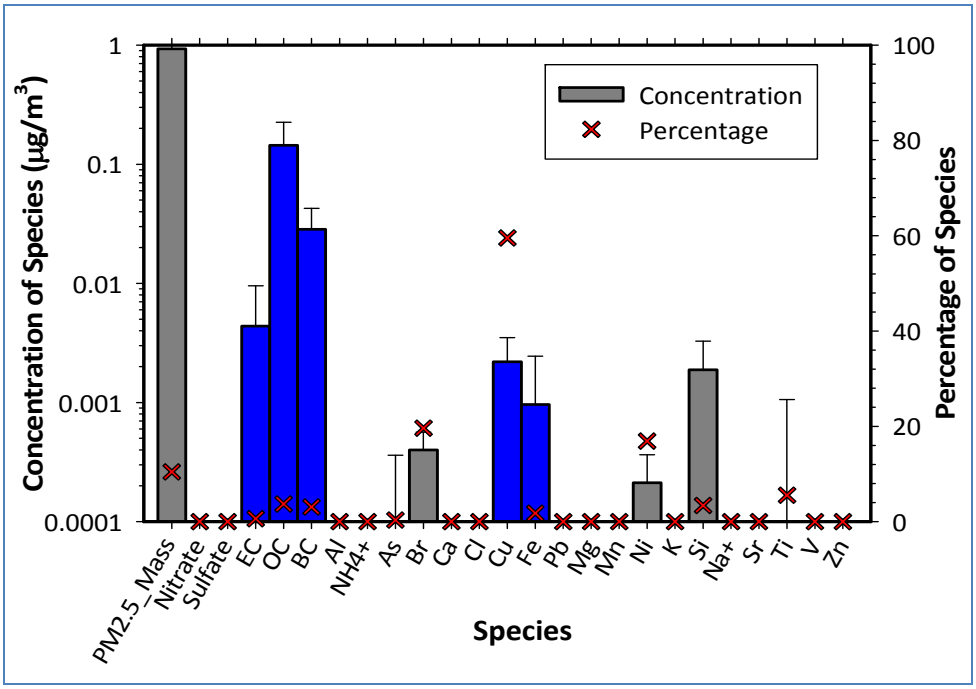


**Figure 4.5(a). PMF profile for gasoline-fired vehicles.** Signature species are shown with blue bars. About 60% of copper (Cu) was apportioned to gasoline vehicles.

In many urban areas, EC is primarily emitted by diesel engines and thus is often used as a tracer for motor vehicle diesel emissions in receptor modeling studies (Solomon et al., 2008). Generally, the concentration of total OC is expected to be higher than the EC concentration in emissions from gasoline-fired vehicles. Conversely, except for diesel vehicles operating at very slow speeds and in stop-and-go traffic, the concentration of total EC is expected to be higher than the OC concentration in emissions from diesel-fired vehicles (Shah et al., 2004; Kim and Hopke, 2008b). Thus, it is possible that emissions from diesel vehicles operating at very slow speeds and in stop-and-go traffic have been included in the gasoline profile because such

emissions have been shown to contain OC/EC concentrations that are comparable to those observed in typical gasoline emissions.

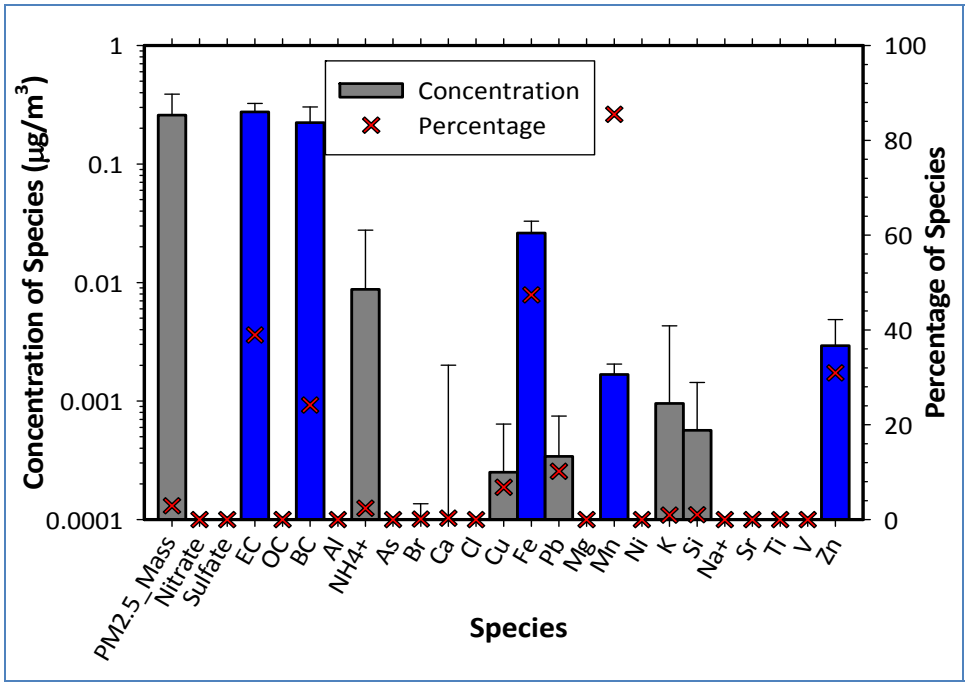


**Figure 4.5(b). PMF profile for diesel vehicles.** About 90% of the measured manganese (Mn) was apportioned to diesel vehicles, along with significant amounts of zinc (Zn), iron (Fe), elemental carbon and black carbon. Signature species are shown with blue bars.

The CPFs for gasoline and diesel vehicles (Figures 4.6(a) and 4.6(b)) are nearly identical suggesting similar potential source locations. The CPFs are observed to point to the directions of the freeway (Interstate-5) as well as major arterial streets and intersections (see Figure 2.1). Although the south-southwestern direction indicated by the motor vehicle CPFs may suggest that mobile source emissions originating from the McChord Air Force Base may have been included in the motor vehicle contributions, the actual impact of the Air Force Base's emissions is expected to be insignificant (EPA, 2008b).

It should be noted that if the analysis were based upon particle number concentrations, it is possible that the resolved relative contributions of motor vehicles would be different. This is because motor vehicles have been reported to emit significant amounts of ultrafine particles (less than 100 nanometers in aerodynamic diameter), which do not weigh as much as the heavier super micron particles (Ogulei et al., 2007). Additionally, because motor vehicles are significant contributors of precursors of secondary aerosol, it is likely that some of the motor vehicle emissions are included in the secondary aerosol contributions.

The total motor vehicle contribution reported in this study (13%) is comparable to the 11% value reported by Kim et al. (2003) in Spokane, WA. Also, Maykut et al. (2003), Wu et al. (2007) and Kim and Hopke (2008a) reported motor vehicle contributions of 10-44% within the Seattle area. But, Jimenez et al. (2006) reported a lower contribution of 2% in the eastern Washington city of

Pullman, WA. A smaller contribution from motor vehicles in Pullman is expected compared to the larger cities with greater vehicle miles traveled.

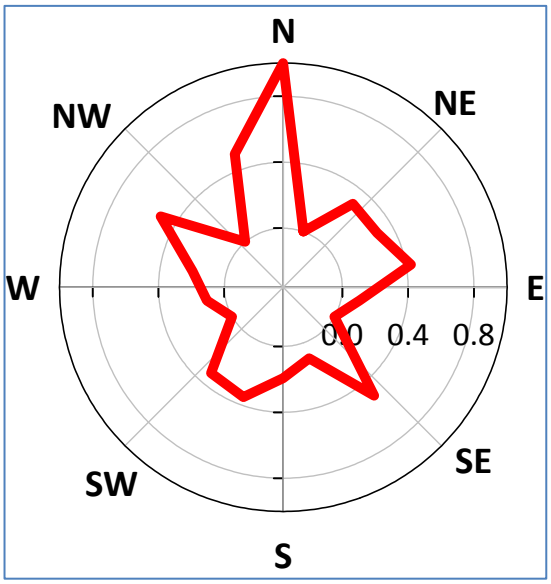


**Figure 4.6(a). CPF for gasoline vehicles.**

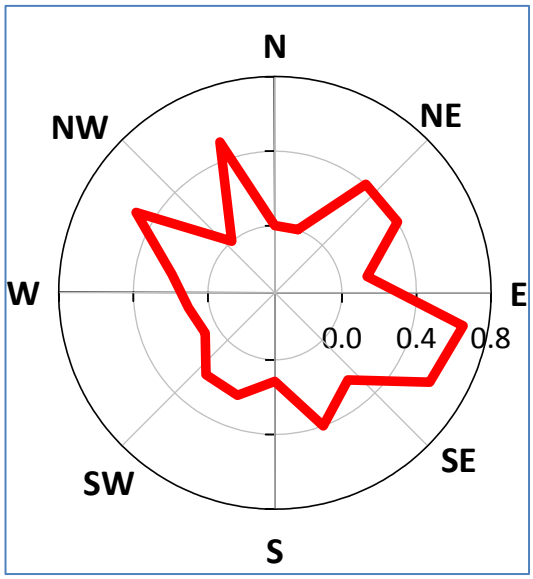


**Figure 4.6(b). CPF for diesel vehicles.**

## 4.3 Secondary Aerosol (Secondary Nitrate and Secondary Sulfate)

Secondary aerosol was dominated by ammonium nitrate, $NH_4NO_3$, and ammonium sulfate, $(NH_4)_2SO_4$. As shown in Section 3.0, secondary aerosol cumulatively accounted for as much as 25% of the average apportioned mass. Figures 4.7(a) and 4.7(b) show the source profiles for secondary nitrate and secondary sulfate, respectively. The measured nitrate and sulfate concentrations were highly correlated with the resolved secondary nitrate and sulfate contributions, with Pearson's correlation coefficients ($r^2$) of 0.96 and 0.89, respectively. The ammonium ion ($NH_4^+$) was also highly correlated with both secondary nitrate and sulfate, with correlation coefficients of 0.86 and 0.84, respectively.

Secondary nitrate in the atmosphere is primarily formed from photochemically-catalyzed atmospheric reactions involving nitrogen oxides (NOx), ammonia and ozone. The CPF for secondary nitrate (Figure 4.8(a)) indicates that the secondary nitrate may have resulted from processing of NOx emissions originating primarily from traffic traveling along I-5 and major arterial streets. The predicted secondary nitrate concentration peaks in the winter and late fall because the combination of high relative humidity and low ambient temperature in the winter promotes partitioning of ammonium nitrate into the particle phase (Moya et al. 2001; Tolocka et al., 2004).

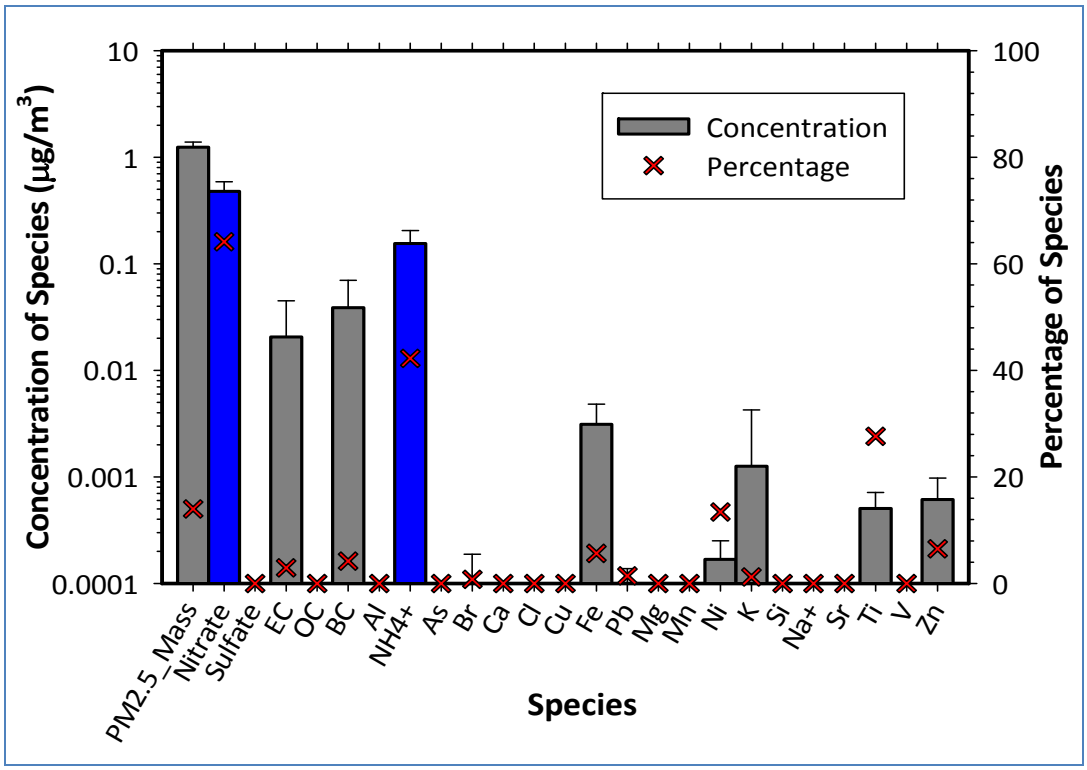


**Figure 4.7(a). PMF source profile for secondary nitrate**. Signature species are shown with blue bars.

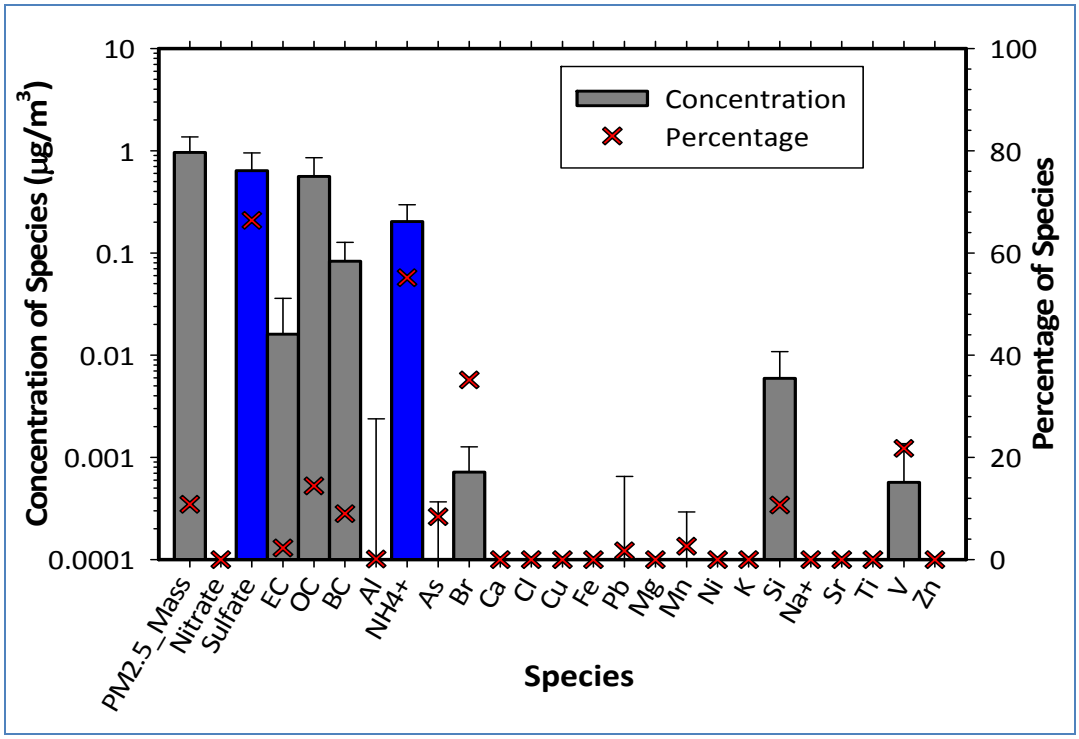


**Figure 4.7(b). PMF source profile for secondary sulfate**. Signature species are shown with blue bars.

Secondary sulfate particles, on the other hand, are largely formed through atmospheric gas phase and aqueous phase reactions involving sulfur dioxide ($SO_2$) and atmospheric oxidants such as the hydroxyl radical (OH), hydrogen peroxide ($H_2O_2$) and ozone. Some of the sulfate particles may also be emitted directly as primary sulfate particles (Kerminen et al. 2000).

The reaction pathways that lead to the formation of secondary nitrate and sulfate also lead to the formation of carbonaceous secondary aerosol. This generally explains the presence of significant amounts of carbonaceous species (primarily OC) in the secondary aerosol profiles (Figures 4.7(a) and 4.7(b)).

The CPF for secondary sulfate does not show a meaningful relationship with the overall wind profile (Figure 2.4). This indicates that the secondary sulfate resolved in this analysis may have primarily been formed from atmospheric processing of locally-generated $SO_2$ emissions, including $SO_2$ emissions from point and non-point sources. This conclusion was further supported by the prevalence of concentration spikes in the secondary nitrate and sulfate time series. Multiple authors have previously reported relatively smooth time series for regionally transported aerosol (e.g., Ogulei et al., 2005). The presence of significant amounts of vanadium, V (20%) and bromine, Br (35%) in the secondary sulfate profile may suggest a significant contribution from ship emissions.

The sulfate time series peaked in late summer and early fall, with the highest average sulfate concentration observed in August. This is attributable to increased photochemical activity close to the monitoring site. In contrast to the sulfate, the nitrate series peaked in the winter and late fall (Figure 4.9). As explained by Seinfeld and Pandis (1998), high ambient concentrations of particulate secondary nitrate (primarily ammonium nitrate) are observed when there is a combination of high relative humidity and low ambient temperature. Our analysis of the area's ambient relative humidity and temperature data, measured during the study period, revealed that

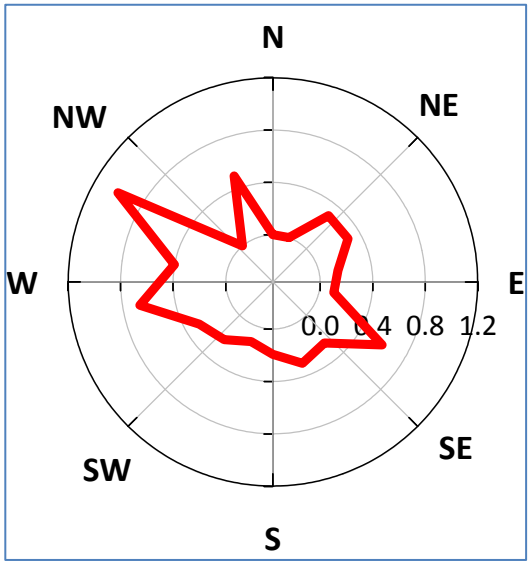


**Figure 4.8(a). CPF for secondary nitrate.**

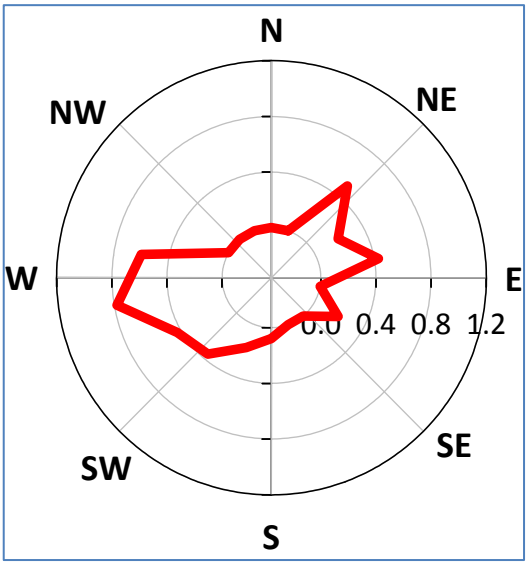


**Figure 4.8(b). CPF for secondary sulfate.**

the highest relative humidity measurements were typically observed between October and February, while the lowest ambient temperatures were observed in January. Thus, while there may be other factors, it is likely that the observed seasonal patterns in sulfate and nitrate concentrations are primarily defined by weather conditions within the study area.

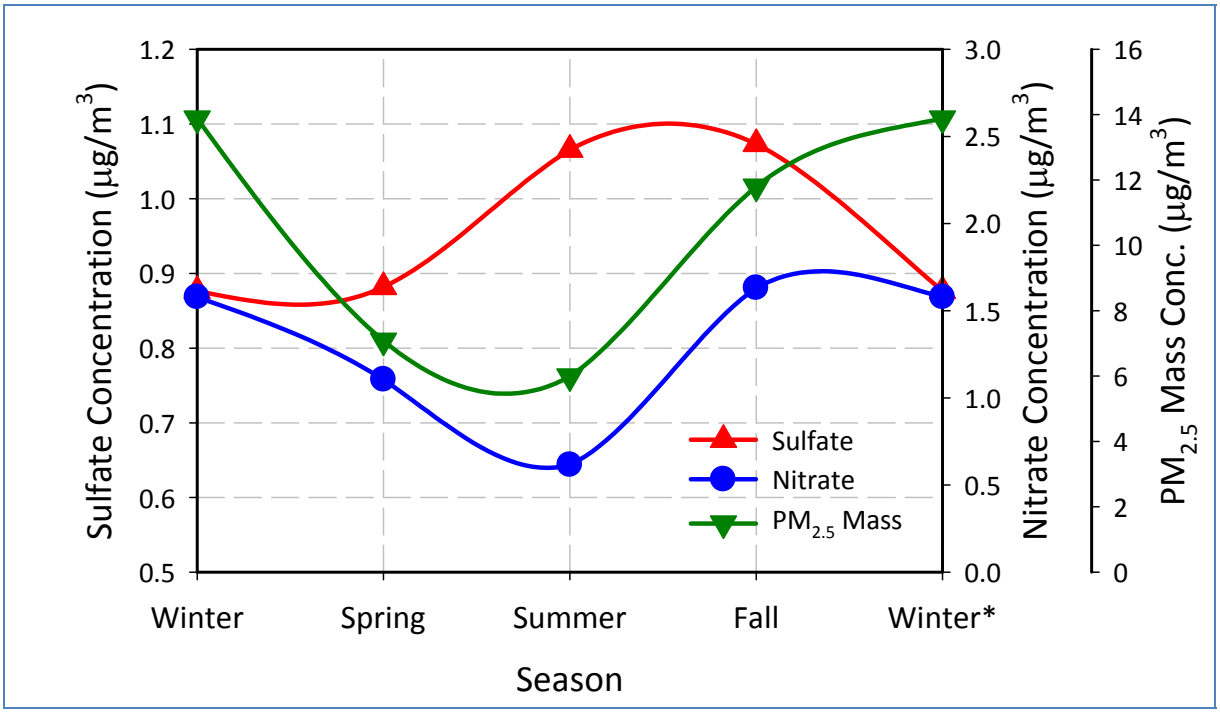


**Figure 4.9. Seasonal profile for secondary aerosol and $PM_{2.5}$ mass.**

It is important to note from Figure 4.9 that the time series for total $PM_{2.5}$ mass is similar to that of secondary nitrate. This may suggest that in addition to weather factors, the primary contributors to the observed nitrate may also be responsible for much of the observed total mass.

The total secondary aerosol contribution (25%) resolved in this study is comparable to published values from major cities in the Pacific Northwest. For example, Kim et al. (2003) and Jimenez et al. (2006) reported total secondary aerosol contributions of 28% in Spokane, WA and 20% in Pullman, WA, respectively. Kim and Hopke (2008a) reported secondary nitrate contributions of 12-26% and secondary sulfate contributions of 17-20% in five sites within the Seattle area. Kim and Hopke (2008b) reported secondary nitrate contributions of 15-16% and secondary sulfate contributions of 15-18% in the Olympic Peninsula, WA; Portland, OR; and Anchorage, AK. While some differences do exist in the actual apportioned contributions in these studies, it is clear that secondary aerosol accounts for a significant portion of the total aerosol burden in many cities in the Pacific Northwest.

## 4.4 Industrial Emissions

Industrial emissions accounted for as much as 90% of the apportioned arsenic (As), 50% of zinc (Zn), and about 50% of lead (Pb) emissions in this study (Figure 4.10). We observed strong

correlations between industrial emissions and total $PM_{2.5}$ mass, organic carbon (OC), black carbon (BC), arsenic (As), lead (Pb) and zinc (Zn), with Pearson's correlation coefficients of 0.81, 0.84, 0.74, 0.86, 0.75 and 0.84, respectively.

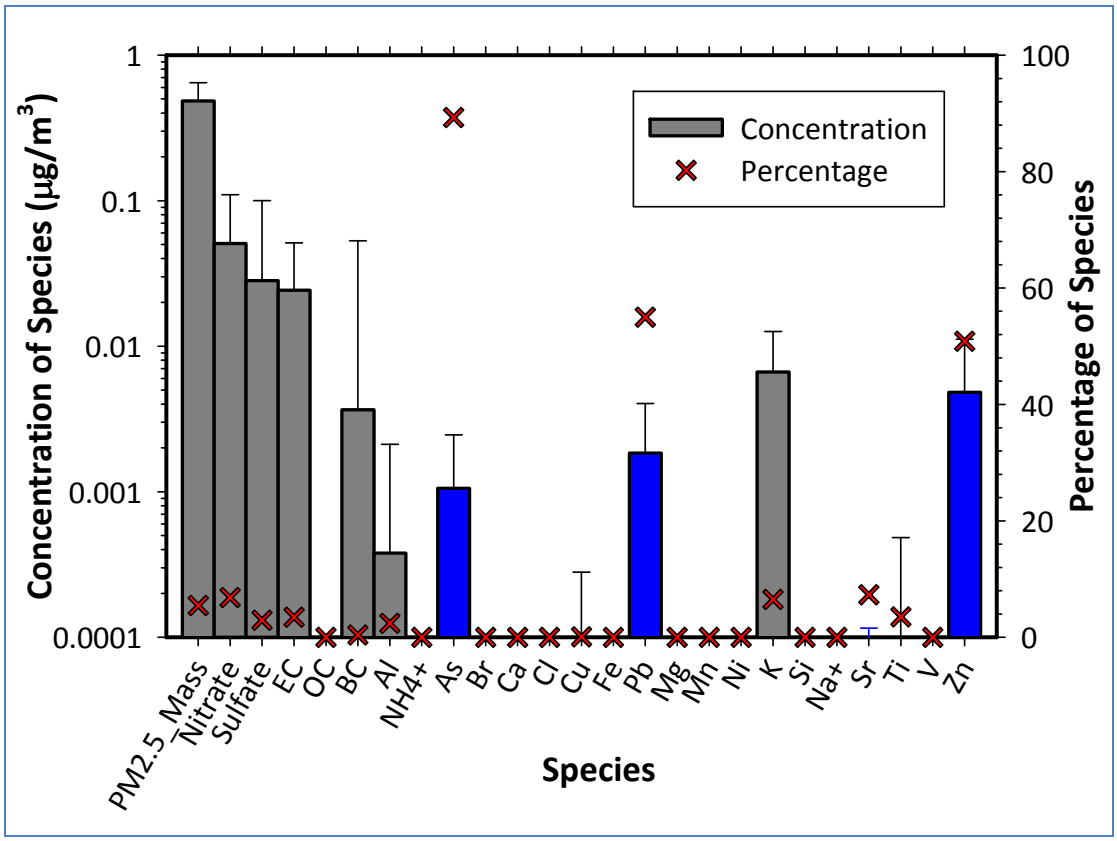


**Figure 4.10. PMF profile for industrial emissions**. Signature species are shown with blue bars.

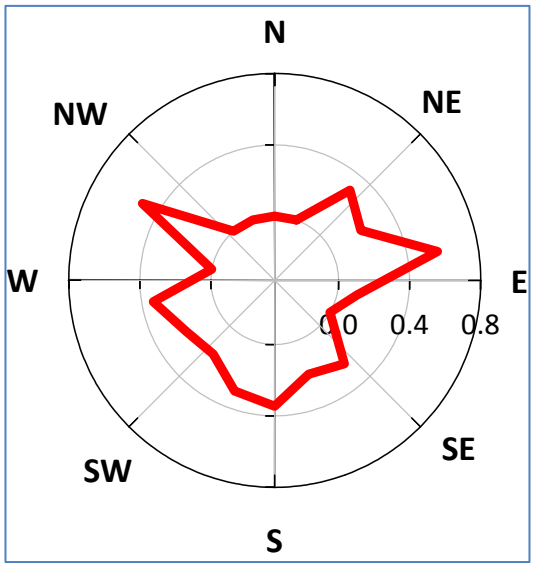


**Figure 4.11. CPF for industrial emissions.**

On average, contributions from industrial emissions were lowest in the summer, probably due to better atmospheric mixing in the summer compared to other times in the year. Also, as shown in Table 3.2, contributions from this source category appeared to decrease annually from their 2006 maximum. This may indicate that existing control measures for point sources might be offsetting the effects of any industrial growth on annual emissions thereby producing measurable reductions in annual emissions. However, more data are needed to verify that this decline is real and that it persists when more years are included in the analysis.

While the CPF (Figure 4.11) suggests the existence of contributing sources in multiple directions, it also

indicates that point sources located to the northeast, and, perhaps, the Port of Tacoma, are partly responsible for the observed mass concentrations at the monitor. The observed strong correlation between these emissions and combustion products such as OC and BC suggests a significant influence of combustion sources.

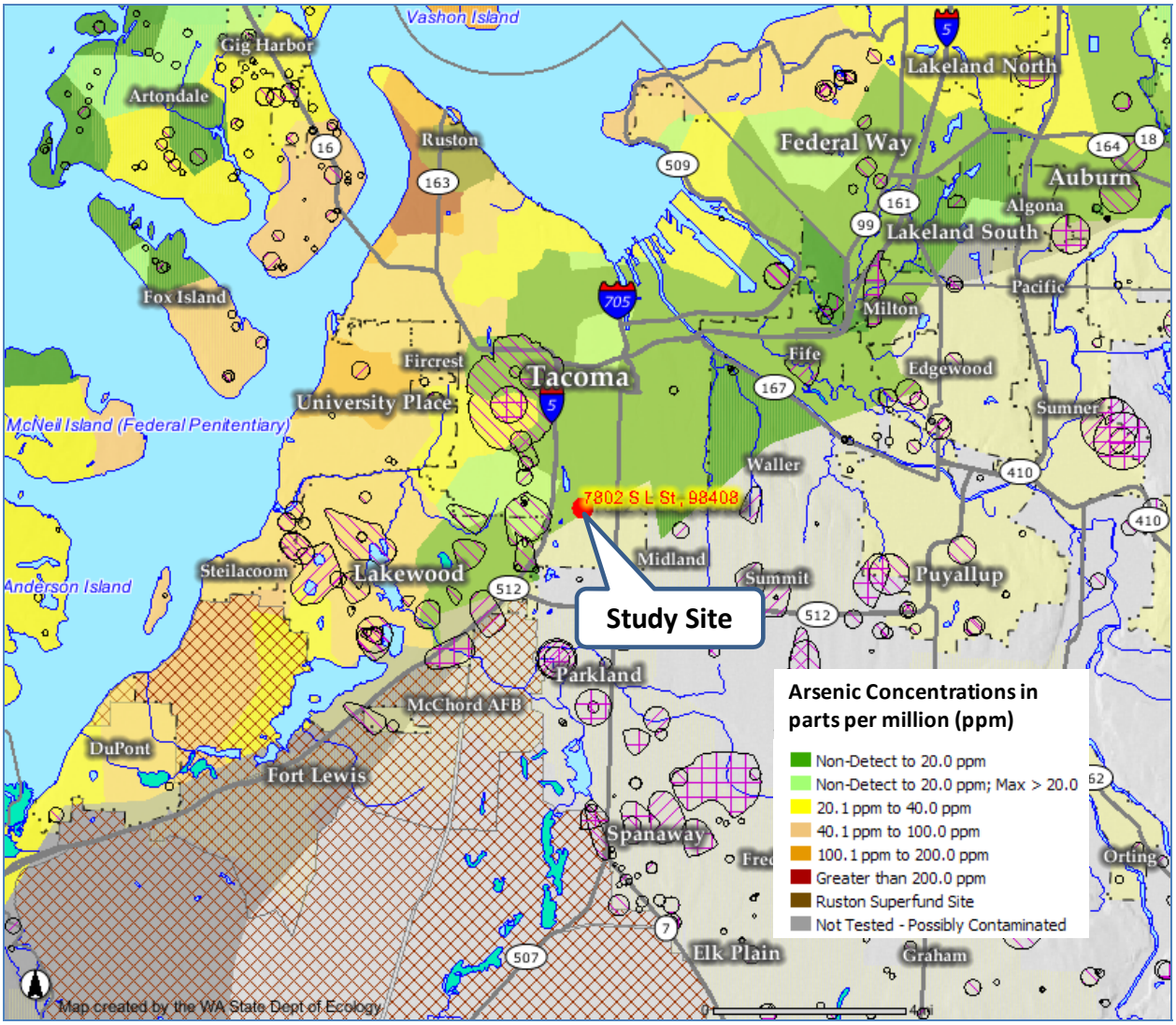


**Figure 4.12. Predicted extent of arsenic contamination due to the ASARCO Smelter** (Department of Ecology Facility/Site Identification System).

The strong correlation with arsenic (As) suggests that the contributions that make up this source may also consist of crustal-laden remnants of the now-defunct ASARCO Tacoma Smelter previously located in the town of Ruston, WA. Figure 4.12 shows the Department of Ecology's prediction of the extent of arsenic contamination as a result of the now-defunct ASARCO Tacoma Smelter. The map shows an estimate of the highest arsenic levels likely to be found in an area, based upon a relatively small number of samples. It can be observed that high arsenic

concentrations are predicted to occur in the southwest, northwest and northeast quadrants relative to the sampling site.

We confirmed through a CPF analysis of the measured ambient air arsenic concentrations that there were no significant arsenic contributions coming from the southeast. The CPF for the measured arsenic concentrations (CPF not shown here) showed that most of the arsenic came from the north-northwest and southwest directions. Thus, the southeast direction shown by the CPF for industrial emissions (Figure 4.11) may suggest the existence of industrial point sources in that direction.

An on-going regional atmospheric deposition study has reported generally higher fluxes of metals (As, Cu, Pb) and total polycyclic aromatic hydrocarbons (PAHs) within Tacoma Commencement Bay (located about 5 miles northeast of the sampling site) than in any of the other Puget Sound area sites being investigated (Brandenberger et al., 2009). While the true sources of the observed heavy metals in our study are unknown, it is likely that background contamination from the now-defunct smelter, coupled with freshly-emitted point and non-point emissions, are responsible for the observed metallic concentrations.

Industrial emissions accounted for about 6% of the overall apportioned mass. This value is in agreement with published contributions from other sites within Washington State. For example, Maykut et al. (2003) reported an average contribution of 7% from "industry" in Beacon Hill (Seattle).

## 4.5 Fugitive Dust

Fugitive dust was characterized by an abundance of crustal elements, aluminum (Al), calcium (Ca), iron (Fe) and silicon (Si). It accounted for about 80% of the apportioned aluminum and 82% of the silicon (Figure 4.13).

Fugitive dust accounted for about 4% of the total apportioned mass. The CPF (Figure 4.14) suggests significant contributions from re-suspended dust from highway and local traffic. Because there is a gravel operation located to the southwest of the sampling site, it is also likely that the southwesterly direction indicated by the CPF indicates contributions from that facility.

Fugitive dust was poorly correlated with total $PM_{2.5}$ mass ($r^2 = 0.19$) indicating that its influence on the measured total mass was not significant. As expected, fugitive dust emissions were highest in the summer and lowest in the winter.

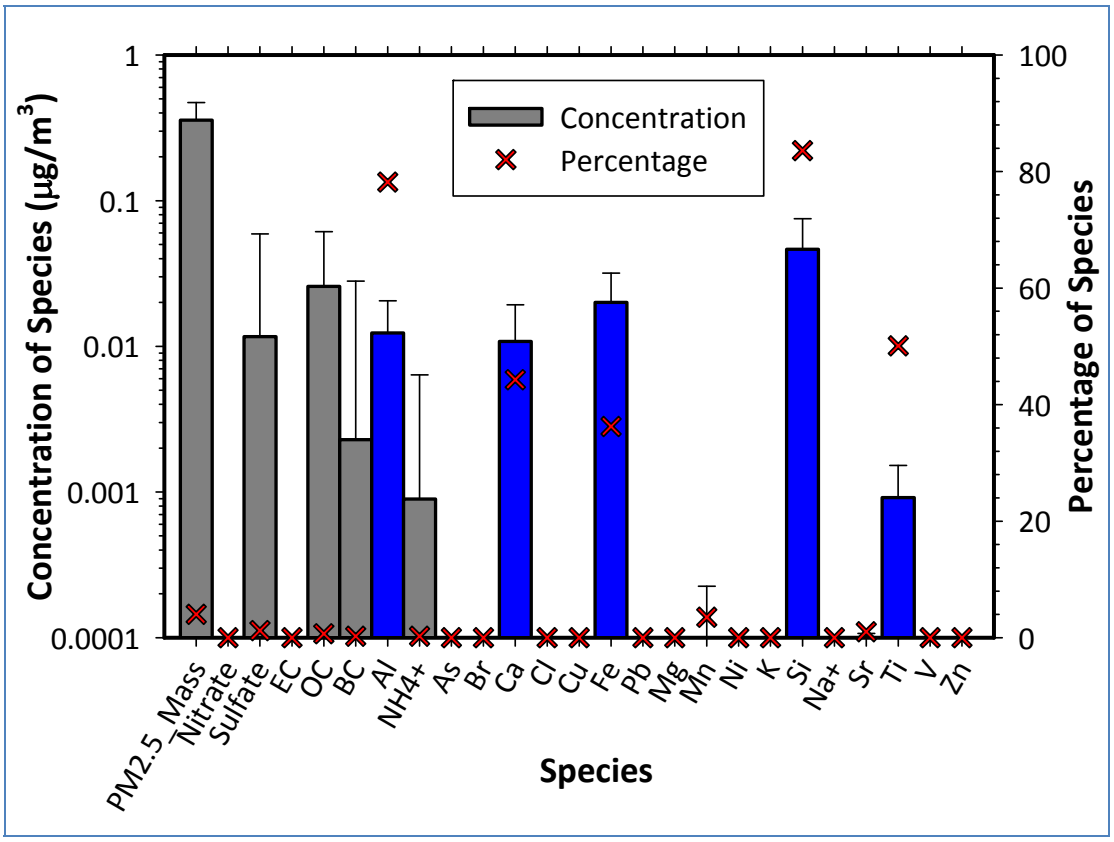


**Figure 4.13. PMF profile for fugitive dust**. Signature species are shown with blue bars.

## 4.6 Oil Combustion and Ships

Oil combustion and ships represent only about 1% of the apportioned mass. They accounted for about 70% of the apportioned nickel (Ni) and 72% of vanadium (V). Ni and V are known markers for oil combustion and emissions from ships. Although the PMF profile (Figure 4.15) indicates the presence of significant concentrations of many species in emissions associated with this source, correlations were generally weak between the oil combustion and ships source with those species. Strong correlations were observed with Ni ($r^2$ = 0.86) and V ($r^2$ = 0.92), while moderate correlations were found with sulfate ($r^2$ = 0.46), calcium, Ca ($r^2$ = 0.58) and iron, Fe ($r^2$ = 0.51). A relatively weak correlation was observed with total

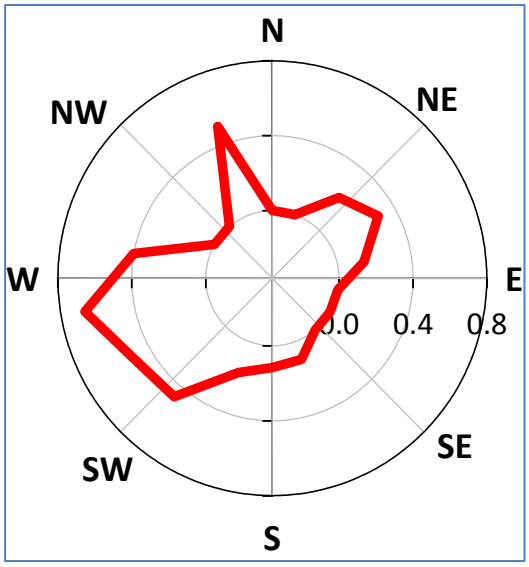


**Figure 4.14. CPF for fugitive dust**.

$PM_{2.5}$ mass ($r^2 = 0.29$), which suggests a relatively insignificant influence by oil combustion/ships on the measured total mass concentrations.

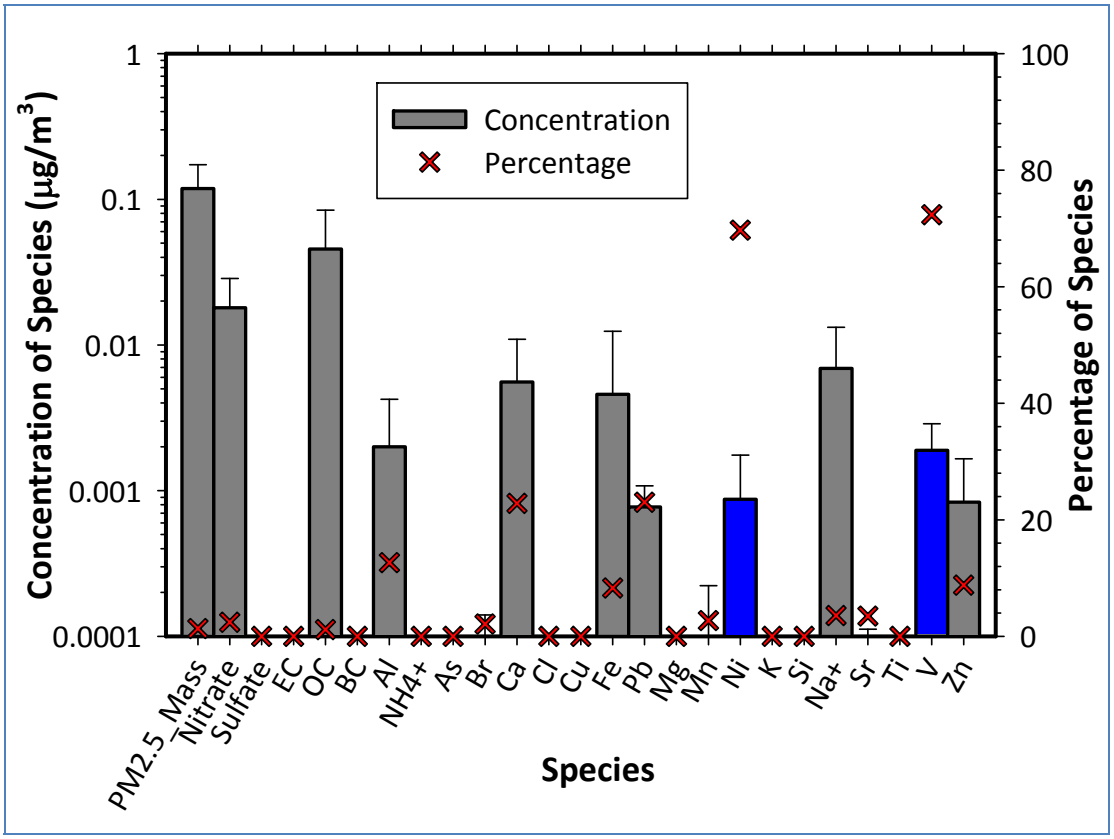


**Figure 4.15. PMF profile for oil combustion/ships.** Signature species are shown with blue bars.

The CPF (Figure 4.16) suggests contributions from multiple directions probably as a result of scattering of residual oil combustion sources as well as wind meandering close to the sampling site. It can also be observed that emissions originating from the Port of Tacoma may have impacted the measured mass concentrations at the sampling site. The southwesterly direction shown by the CPF may indicate ship emissions being blown offshore by southwesterly winds. The CPF also indicates the presence of significant oil combustion contributions from the northwest and southwest directions.

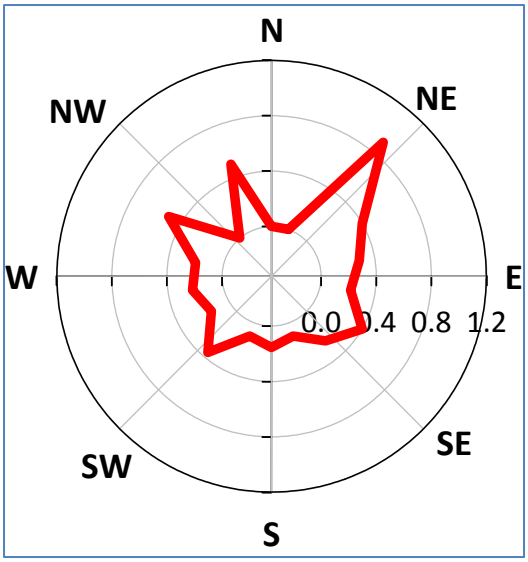


**Figure 4.16. CPF for oil combustion and ships.**

The contribution from oil combustion/ships resolved in this analysis is less than the value reported from other study sites in Washington State. Kim and Hopke (2008a) reported average oil

combustion contributions of 4-6% in five sites within the Seattle area. The authors suggested that a major portion of the oil combustion emissions may be attributable to ships operating within the Port of Seattle. In a related study, Kim and Hopke (2008b) reported an oil combustion contribution of 19% in the Olympic Peninsula, primarily attributable to ship emissions.

The averaged contribution from oil combustion/ships generally peaked in August or September. Although shipping activity within the Port of Tacoma fluctuates throughout the year, increased shipping activity in late summer/early fall was reported by the Pacific Maritime Association during the study period (PMA, 2009). Thus, shipping activity within the Port of Tacoma may have been responsible for much of the contributions apportioned to this source category.

## 4.7 Other Sources

Other emission sources resolved in this analysis include fireworks, freshly-emitted sea salt and processed (aged) sea salt. These sources cumulatively accounted for about 6% of the apportioned mass, with individual contributions of 2%, 4% and 0.3%, respectively. Neither of these sources had a meaningful correlation with $PM_{2.5}$ mass indicating that their influence on the measured total mass concentrations was insignificant. Figure 4.17 shows PMF source profiles for fireworks, freshly-emitted sea salt and aged sea salt. The corresponding CPFs are shown in Figure 4.18.

The primary identifying species for fireworks are strontium (Sr) and potassium (K). Fireworks were highly correlated with copper, Cu ($r^2 = 0.89$), magnesium, Mg ($r^2 = 0.71$), potassium, K ($r^2 = 0.89$), and strontium, Sr ($r^2 = 0.86$). The time series for the resolved fireworks source (Figure 4.19) confirmed that fireworks displays associated with Independence Day celebrations were the primary contributors to the resolved fireworks emissions. The CPF for fireworks (Figure 4.18(a)) indicates that fireworks emissions mostly originated from the northwest and southwest of the sampling site. A literature review revealed no source apportionment data for fireworks, presumably because most source apportionment studies have typically omitted fireworks data from their analyses.

Fresh sea salt was identified by the predominance of the chloride ion ($Cl^-$), sodium ion ($Na^+$) and magnesium (Mg). About 97% of the $Cl^-$ was apportioned to freshly-emitted sea salt. The CPF (Figure 4.18(b)) is consistent with sea salt emissions that are blown offshore by strong predominantly southwesterly winds.

Aged sea salt is characterized by high sodium ($Na^+$), magnesium (Mg) and calcium (Ca) concentrations, accompanied by no chloride ($Cl^-$) or other halogens. In this case, the chloride has been substituted by nitrate ($NO_3^-$) through atmospheric reaction with nitric acid ($HNO_3$). In contrast to fresh sea salt, aged sea salt contributions were highest in the summer probably because aged sea salt particles have been reported to associate with sulfate particles (Zhuang et al., 1999).

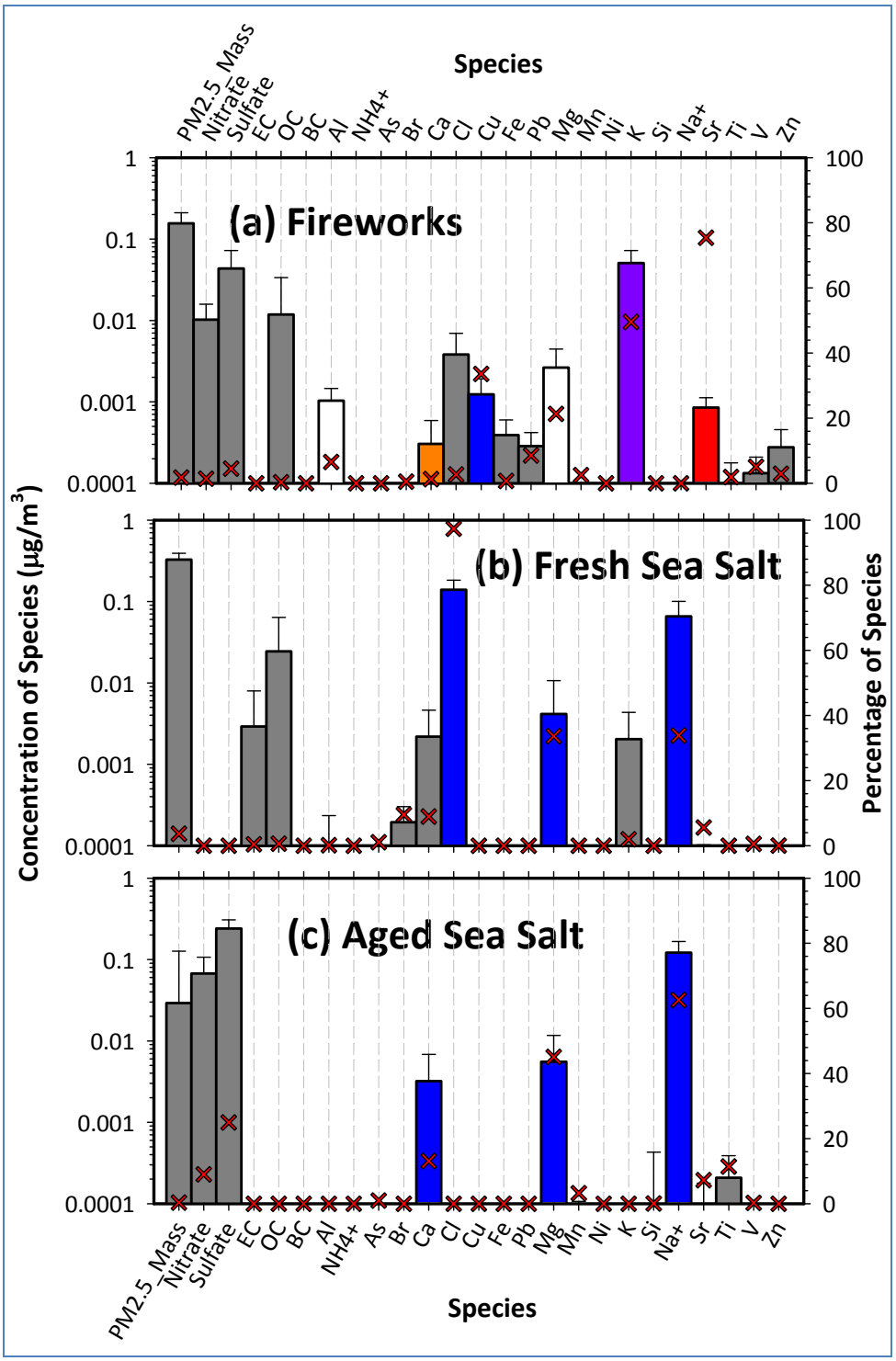


**Figure 4.17. PMF profiles for (a) fireworks, (b) freshly-emitted sea salt, and (c) processed (aged) sea salt.** Bars are concentrations and a red cross in the chart is the percentage of that species apportioned to that source. Non-gray colors in the fireworks profile represent typical colors of those elements in a typical fireworks display. Blue color bars in other source profiles indicate "marker" species.

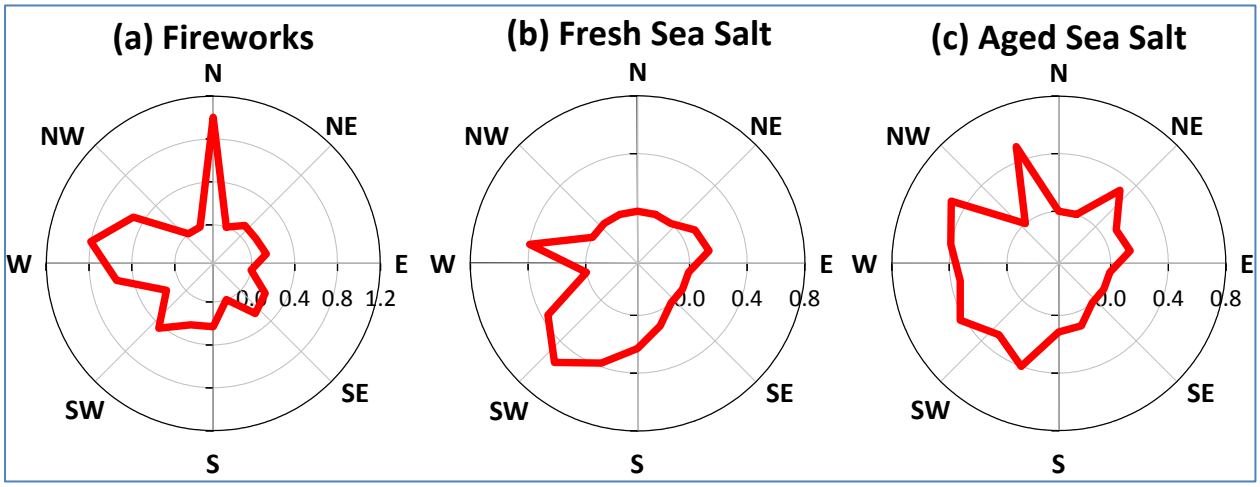


**Figure 4.18. CPFs for (a) Fireworks, (b) Freshly emitted sea salt, and (c) Processed ("aged") sea salt.**

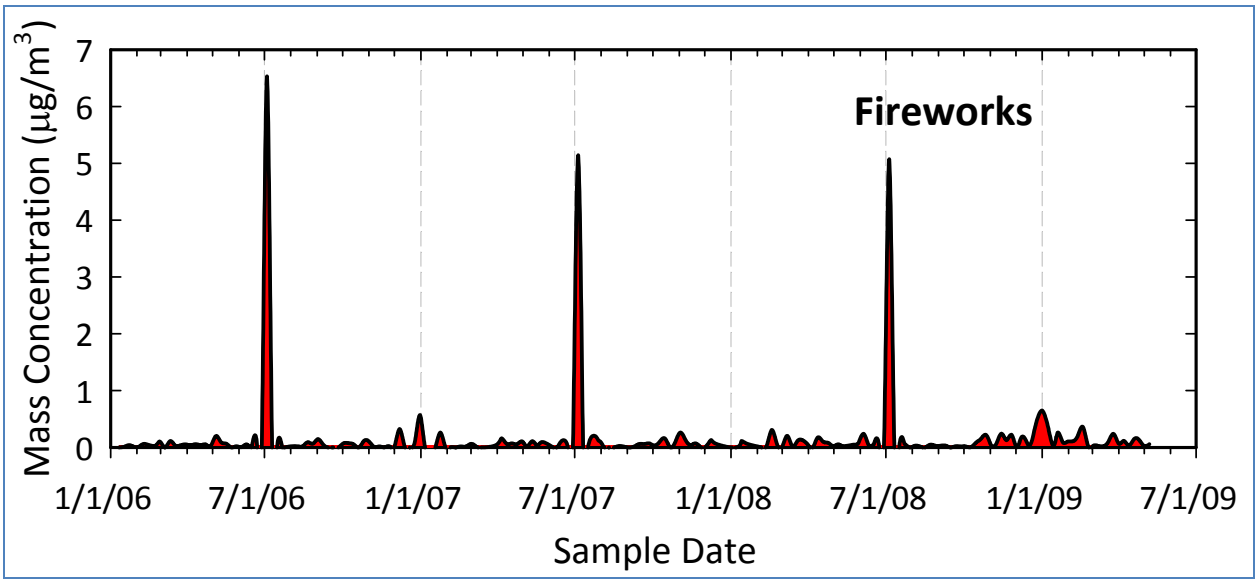


**Figure 4.19. Time series for fireworks.** The contributions were dominated by Independence Day fireworks displays.

The contribution from freshly-emitted sea salt is comparable to contributions found in the technical literature, but the contribution estimate for aged sea salt is lower than the published contributions. For example, Kim and Hopke (2008a) reported aged sea salt contributions of 4-12% and fresh sea salt contributions of 2-4% in five sites within the Seattle area. Additionally, Kim and Hopke (2008b) reported aged sea salt contributions of 5-10% and fresh sea salt contributions of 2-10% within the Olympic Peninsula, WA, Portland, OR and Anchorage, AK. Wu et al. (2007) found a "marine" source (approximately 1-2% of the total mass) and an "aged sea salt" source (approximately 5-6% of the total mass) in Beacon Hill (Seattle).

# 5.0 CONCLUSION

By analyzing the measured elemental species concentrations in Tacoma, Washington, this study has determined that the most significant sources of ambient fine particles in the nonattainment area are wood smoke, gasoline vehicles, diesel vehicles, fugitive dust, fireworks, secondary nitrate, secondary sulfate, oil combustion and ships, arsenic-rich industrial emissions, freshly-emitted sea salt, and processed (aged) sea salt. On average, these sources explained more than 90% of the measured average mass concentration.

The single most dominant source of fine particles in the nonattainment area is wood smoke. We believe that the resolved wood smoke contributions represent combined contributions from wood stoves and other wood-fired home heating devices. Wood smoke contributions had the strongest relationship with the measured total $PM_{2.5}$ mass which illustrates that wood smoke contributions were responsible for the majority of the observed trend in total $PM_{2.5}$ mass concentrations. The source apportionment results showed that wood smoke accounts for nearly one-half of the total measured $PM_{2.5}$ mass on most days. The wood smoke contributions were most significant during the winter and on days when the measured daily $PM_{2.5}$ mass concentration exceeded 20 or 30 $\mu g/m^3$.

Wind direction and wind speed were found to be a factor in the observed wood smoke concentrations. Accordingly, the most significant sources of wood smoke appeared to be those that were located to the southerly and southeasterly directions with respect to the sampling site.

We observed a strong presence of secondary aerosol in the study area. About 25% of the ambient $PM_{2.5}$ mass concentrations were attributable to secondary aerosol. Further analyses identified the resolved secondary aerosol as locally-generated aerosol from multiple local sources of nitrogen oxides, sulfur dioxide and volatile organic compounds. This indicates that a complete emissions control strategy would also consider evaluating local sources of precursors for secondary aerosol, including mobile and non-mobile sources of nitrogen oxides, sulfur dioxide and volatile organic compounds.

We attributed a small but significant portion of the observed $PM_{2.5}$ mass to industrial emissions (roughly 6%). Industrial emissions were rich in arsenic, lead, and zinc. Further analyses revealed that these emissions might be a combination of background/re-suspended emissions from the now-defunct ASARCO Smelter and emissions from active major industries located within the Port of Tacoma.

Finally, our results show that average contributions attributable to wood smoke and local industry appear to have declined approximately linearly, on an annual basis, since the year 2006. We did not see a similar decline with other sources or with the $98^{th}$ percentile wood smoke contributions. Because of the limited time period, it was not possible to verify whether or not the observed decline constitutes a trend. Nonetheless, it is possible that existing control strategies for wood smoke and industrial sources may be creating measurable annual emissions reductions. A follow-up detailed study which includes several years of ambient data may be necessary to

determine the true effect of existing control strategies on annual $PM_{2.5}$ emissions. However, in order to reduce ambient fine particle mass concentrations on specific days, a combination of targeted source- and location-specific emissions reductions and careful forecasting of meteorological conditions may be required.

# 6.0 REFERENCES


Ashbaugh, L.L., Malm, W.C., and Sadeh, W.Z. (1985). A Residence Time Probability Analysis of Sulfur Concentrations at Grand Canyon National Park. Atmospheric Environment 19, 1263–1270.

Brandenberger, J., Gill, G., Crecelius, E., Louchouarn, P., and Kuo, L.-J. (2009). Study of Atmospheric Deposition of Air Toxics to the Waters of Puget Sound: Year One Data Report. Report No. PNWD-4091, August 2009.

EPA (2008a). EPA Positive Matrix Factorization (PMF) 3.0 Fundamentals & User Guide. United States Environmental Protection Agency, Office of Research and Development, Washington, DC., July 2008.

EPA (2008b). EPA Technical Analysis for Tacoma (Pierce County), Washington. http://www.epa.gov/pmdesignations/2006standards/rec/letters/10_WA_EPAMOD.pdf. Last Accessed December 18, 2009.

Hopke, P.K., Lamb, R.E., and Natusch, D.F.C. (1980). Multielemental Characterization of Urban Roadway Dust. Environmental Science & Technology 14, 164–172.

Huang, Y.-C., and Ghio, A. J. (2009). Controlled Human Exposures to Ambient Pollutant Particles in Susceptible Populations. Environmental Health 8(33), 1-10.

Jimenez, J., Wu, C.-F, Claiborn, C., Gould, T., Simpson, C. D., Larson, T.V., and Liu, L.-J. S. (2006). Agricultural Burning Smoke in Eastern Washington—Part I: Atmospheric Characterization. Atmospheric Environment 40, 639-650.

Kerminen,V. M., Pirjola, L., Boy, M., Eskola, A., Teinnila, K., Laakso, L., Asmi, A., Hienola, J., Lauri, A., Vainio, V., Lehtinen, K., and Kulmala, M. (2000). Interaction Between $SO_2$ and Submicron Atmospheric Particles. Atmospheric Environment 52, 41–57.

Kim, E., Larson, T.V., Hopke, P.K., Slaughter, C., Sheppard, L. E., and Claiborn, C. (2003). Source Identification of $PM_{2.5}$ in An Arid Northwest U.S. City By Positive Matrix Factorization. Atmospheric Research 66, 291-305.

Kim, E., and Hopke, P.K. (2008a). Source Characterization of Ambient Fine Particles at Multiple Sites in the Seattle Area. Atmospheric Environment 42, 6047–6056.

Kim, E., and Hopke, P.K. (2008b). Characterization of Ambient Fine Particles in the Northwestern Area and Anchorage, Alaska. Journal of the Air & Waste Management Association 58, 1328–1340.

Lewis, C.W., Norris, G.A., Henry, R.C., and Conner, T.L. (2003). Source Apportionment of Phoenix $PM_{2.5}$ Aerosol with the Unmix Receptor Model. Journal of the Air & Waste Management Association 53, 325-338.

Lewtas, J. (2007). Air pollution combustion emissions: Characterization of Causative Agents and Mechanisms Associated with Cancer, Reproductive, and Cardiovascular Effects. Mutation Research 636, 95–133.

Maykut, N. N., Lewtas, J., Kim, E., and Larson, T.V. (2003). Source Apportionment of $PM_{2.5}$ At An Urban IMPROVE Site in Seattle, Washington. Environmental Science & Technology 37, 5135-5142.

Moya, M., Ansari, A., and Pandis, S. N. (2001). Partitioning of Nitrate and Ammonium Between the Gas and Particulate Phases During the 1997 IMADAAVER Study in Mexico City. Atmospheric Environment 35, 1791–1804.

Ogulei, D., Hopke, P.K., Zhou, L., Paatero, P., Park, S.S., Ondov, J.M., 2005. Receptor Modeling For Multiple Time-Resolved Species: The Baltimore Supersite. Atmospheric Environment 39, 3751–3762.

Ogulei, D., Hopke, P.K., and Wallace, L.A. (2006). Analysis of Indoor Particle Size Distributions in an Occupied Townhouse Using Positive Matrix Factorization. Indoor Air 16, 204-215.

Ogulei, D., Hopke, P.K., Ferro, A.R., and Jaques, P.A. (2007). Factor Analysis of Submicron Particle Size Distributions near a Major United States–Canada Trade Bridge. Journal of the Air & Waste Management Association 57, 190–203.

Onstad, G., and Simpson, C. (2008). Final Report: Measurement of the Contribution of Biomass Combustion to $PM_{2.5}$. Puget Sound Clean Air Agency, Seattle, WA., September 30, 2008.

Paatero, P., and Tapper, U. (1994). Positive Matrix Factorization: A Non-Negative Factor Model with Optimal Utilization of Error Estimates of Data Values. Environmetrics 5, 111-126.

Paatero, P. (1997). Least Squares Formulation of Robust Non-Negative Factor Analysis. Chemometrics and Intelligent Laboratory Systems 37, 23-35.

PMA (2009). Pacific Maritime Association Research Reports. http://www.pmanet.org/hours_data/index.cfm. Last accessed December 18, 2009.

Pope III, C.A. (1996). Adverse Health Effects of Air Pollutants in a Nonsmoking Population. Toxicology 111, 149-155.

Ramadan, Z., Song, X.-H., and Hopke, P.K. (2000). Identification of Sources of Phoenix Aerosol By Positive Matrix Factorization. Journal of the Air & Waste Management Association 50, 1308-1320.

Seinfeld, J. H., and Pandis, S. N. (1998). Atmospheric Chemistry and Physics: From Air Pollution to Climate Change. John Wiley and Sons, New York, p.531–539.

Shah, S.D., Cocker, D.R., Miller, J.W., and Norbeck, J.M. (2004). Emission Rates of Particulate Matter and Elemental and Organic Carbon from In-Use Diesel Engines. Environmental Science & Technology 38, 2544-2550.

Solomon, P.A., Hopke, P.K., Froines, J., and Scheffe, R. (2008). Key Scientific Findings and Policy- and Health-Relevant Insights from the U.S. Environmental Protection Agency's Particulate Matter Supersites Program and Related Studies: An Integration and Synthesis of Results. Journal of the Air & Waste Management Association 58, S-3-S-92, Supplement 2008.

Tolocka, M. P., Lake, D. A., Johnston, M.V., and Wexler,A. S. (2004). Ultra Fine Nitrate Particle Events in Baltimore Observed By Real-Time Single Particle Mass Spectrometry. Atmospheric Environment 38, 3215–3223.

Wu, C.-F, Larson, T.V., Wu, S., Williamson, J., Westberg, H. H., and Liu, L.-J. S. (2007). Source Apportionment of $PM_{2.5}$ and Selected Hazardous Air Pollutants in Seattle. Science of the Total Environment 386, 42–52.

Zhuang, H., Chan, C.K., Fang, M., Wexler, A.S. (1999). Formation of Nitrate and Non-Sea-Salt Sulfate on Coarse Particles. Atmospheric Environment 33, 4223–4233.

# Acronyms and Abbreviations

| | |
|---|---|
| Al | Aluminum |
| As | Arsenic |
| BC | Black Carbon |
| Br | Bromine |
| Ca | Calcium |
| Cl | Chlorine |
| $Cl^-$ | Chloride Ion |
| Co | Cobalt |
| CPF | Conditional Probability Function |
| Cr | Chromium |
| Cu | Copper |
| EC | Elemental Carbon |
| Ecology | Washington State Department of Ecology |
| EPA | United States Environmental Protection Agency |
| Fe | Iron |
| FRM | Federal Reference Method |
| Hg | Mercury |
| K | Potassium |
| $K^+$ | Potassium ion |
| Mg | Magnesium |
| Mn | Manganese |
| N | Number of valid samples |
| Na | Sodium metal |
| $Na^+$ | Sodium Ion |
| NAAQS | National Ambient Air Quality Standard |
| $NH_4^+$ | Ammonium ion |
| Ni | Nickel |
| $NO_3^-$ | Nitrate ion |
| NOx | Nitrogen oxides |
| OC | Organic Carbon |
| Pb | Lead |
| $PM_{2.5}$ | Particulate matter with an aerodynamic diameter less than or equal to 2.5 micrometers |
| PMF | Positive Matrix Factorization |
| PSCAA | Puget Sound Clean Air Agency |
| Rb | Rubidium |

| | |
|---|---|
| S | Sulfur |
| Se | Selenium |
| Si | Silicon |
| SIP | State Implementation Plan |
| $SO_2$ | Sulfur dioxide |
| $SO_4^{2-}$ | Sulfate ion |
| Sr | Strontium |
| STN | Speciation Trends Network |
| Ti | Titanium |
| TOR | Thermal Optical Reflectance |
| TOT | Thermal Optical Transmittance |
| V | Vanadium |
| Zn | Zinc |
| $\mu g/m^3$ | Micrograms per cubic meter of ambient air |